Aus der Klinik für Dermatologie
der Heinrich-Heine-Universität Düsseldorf
Direktor: Univ.-Prof. Dr. med. Bernhard Homey

Systematische Analysen der Effekte boviner Hyaluronidase auf strukturelle Zellen der Haut

Dissertation

zur Erlangung des Grades eines Doktors der Medizin
der Medizinischen Fakultät der Heinrich-Heine-Universität Düsseldorf

vorgelegt von
Bettina Alexandra Buhren
2022

Als Inauguraldissertation gedruckt mit der Genehmigung der
Medizinischen Fakultät der Heinrich-Heine-Universität Düsseldorf

gez.:
Dekan: Prof. Dr. med. Nikolaj Klöcker
Erstgutachter: Prof. Dr. med. Peter Arne Gerber
Zweitgutachter: Prof. Dr. med. Timm J. Filler

Für meine Familie.

Teile dieser Arbeit wurden veröffentlicht:

Buhren, B. A., Schrumpf, H., Gorges, K., Reiners, O., Bölke, E., Fischer, J. W., Homey, B., Gerber, P. A., (2020), Dose- and time-dependent effects of hyaluronidase on structural cells and the extracellular matrix of the skin. *European Journal of Medical Research*, (25) 60 – 71.

Summary

The enzyme hyaluronidase (HYAL) cleaves its substrate hyaluronic acid (hyaluronan; HA) generating fragments with size specific and widely differing cell specific activities. However, the molecular and cellular effects of applied HYAL on the physiological HA metabolism as well as the structural cells of the skin have not been fully elucidated.

The aim of this work was the analysis of dose- and time-dependent molecular and cellular effects of HYAL on structural cells and HA metabolism of the skin. For this purpose, chip-based, genome-wide expression analyses (Affymetrix GeneChip® PrimeView™ human gene expression arrays), quantitative real-time polymerase chain reaction (RT-PCR) analyses, enzyme-linked immunosorbent assays (ELISA), immunohistochemical staining (DAB), and *in vitro* wound healing assays were used to characterize the dose-dependent and time-kinetic effects of HA and HYAL on human dermal fibroblasts (NHDF), primary human epidermal keratinocytes (HEK) and *ex vivo* cultured skin biopsies.

Stimulation of NHDF with HA and HYAL showed up to 1.8-fold induced expression of HA synthases (HAS) in genome-wide expression analyses. In a cutaneous *in vitro* wound healing model, the addition of HA and HYAL resulted in significantly accelerated wound closure. Furthermore, HYAL induced HAS1 and HAS2 mRNA gene expression in NHDF. Strikingly, the application of HYAL in low concentrations lead to a significantly higher induction of HAS compared to medium and high concentrations of HYAL. This observation correlated with elevated HA levels measured by ELISA in supernatants of HYAL-stimulated NHDF, with the highest HA levels detected after addition of HYAL at low concentration. Finally, in immunohistochemical analyses the addition of HYAL at low concentrations resulted in a pronounced HA accumulation in *ex vivo* cultured skin biopsies, while high concentrations of HYAL reduced dermal HA levels.

Zusammenfassung

Das Enzym Hyaluronidase (HYAL) spaltet sein Substrat, die Hyaluronsäure (Hyaluronan; HA), in kleinere größenspezifische Fragmente, die sich durch unterschiedliche zellspezifische Eigenschaften auszeichnen. Die molekularen und zellulären Effekte applizierter HYAL auf die Regulation des HA-Metabolismus sowie auf strukturelle Zellen der Haut wurden bis dato nur unzureichend untersucht.

Das Ziel dieser Arbeit war es, die dosis- und zeitabhängigen molekularen und zellulären Effekte von HYAL auf strukturelle Zellen sowie den HA-Metabolismus der Haut zu analysieren. Dazu wurden Chip-basierte, genomweite Expressionsanalysen (*Affymetrix GeneChip® PrimeView™ Human Gene Expression Arrays*), quantitative *Real-Time* Polymerasekettenreaktion (RT-PCR)-Analysen, *Enzym-Linked Immunosorbent Assays* (ELISA), immunhistochemische Färbungen (DAB) und *in vitro*-Wundheilungsassays durchgeführt, um die dosisabhängigen und zeitkinetischen Effekte von HA und HYAL auf humane dermale Fibroblasten (NHDF), primäre humane epidermale Keratinozyten (HEK) sowie *ex vivo* kultivierte Hautbiopsien näher zu charakterisieren.

In genomweiten Expressionsanalysen zeigte die Stimulation von NHDF mit HA und HYAL eine bis zu 1,8-fach induzierte Expression von HA-Synthetasen (HAS). In einem kutanen *in vitro*-Wundheilungsmodell führte die Zugabe von HA und HYAL zu einem signifikant beschleunigten Wundverschluss. Darüber hinaus induzierte HYAL in NHDF die HAS1- und HAS2-mRNA-Genexpression. Interessanterweise führte die Anwendung von HYAL in niedrigen Konzentrationen im Vergleich zu mittleren und hohen Konzentrationen zu einer signifikant höheren Induktion von HAS. Diese Beobachtung korrelierte mit erhöhten, mittels ELISA gemessenen HA-Konzentrationen in Überständen HYAL-stimulierter NHDF, wobei die höchsten HA-Konzentrationen nach Zugabe niedrig-dosierter HYAL detektiert wurden. In immunhistochemischen Analysen zeigte sich schließlich, dass die Zugabe von HYAL in niedrigen Konzentrationen zu einer ausgeprägten HA-Akkumulation in *ex vivo* kultivierten Hautbiopsien führte, während hohe Konzentrationen von HYAL die dermale HA-Menge reduzierten.

Abbreviations

BSA	Bovine serum albumin
CD44	Cluster determinant 44
cDNA	Complementary deoxyribonucleic acid
CTRL	Control
Da	Dalton
DAB	3,3'-diaminobenzidine
dT	Deoxy-thymidine
ECM	Extracellular matrix
EDC	Epidermal differentiation complex
EDTA	Ethylenediaminetetraacetic acid
EGF	Epidermal growth factor
EGFR	Epidermal growth factor receptor
ELISA	Enzyme-linked immunosorbent assay
FC	Fold change
FCS	Fetal calf serum
GAG	Glycosaminoglycan
GalNAc	*N*-acetylgalactosamine
GlcA	Glucuronic acid
GlcNAc	*N*-acetylglucosamine
h	Hour
HA	Hyaluronan
HABP1	Hyaluronan-binding protein 1
HaCaT	Spontaneously immortalized human keratinocyte line
HAS	HA synthase
HBEGF	Heparin-binding EGF-like growth factor
HEK	Human epidermal keratinocytes
HMW-HA	High molecular weight HA
HRP	Horseradish peroxidase
HYAL	Hyaluronidase
IL	Interleukin

LCE	Late cornified envelope gene cluster
LMW-HA	Low molecular weight HA
MMP	Matrix metalloproteinases
MMW-HA	Medium molecular weight HA
M_r	Relative molecular mass
mRNA	Messenger ribonucleic acid
NHDF	Normal human dermal fibroblasts
OD	Optical density
PBS	Phosphate-buffered saline
PCR	Polymerase chain reaction
PG	Proteoglycan
pH	Potentia hydrogenii
qPCR	Quantitative PCR
RHAMM	Receptor for hyaluronic-acid-mediated motility
RIN	RNA integrity number
RMA	Robust multi-array average
RNA	Ribonucleic acid
ROS	Reactive oxygen species
rRNA	Ribosomal ribonucleic acid
RT-PCR	Real-time PCR
SEM	Standard error of the mean
SFM	Serum-free medium
SPAM1	Sperm adhesion molecule 1
TBS	Tris-buffered saline
TGFA	Transforming growth factor alpha
U	Unit
UVB	Ultraviolet B

Table of contents

1. Introduction

1.1 Human skin

As the largest organ of the body, human skin accounts for approximately 15% of total body weight (Kanitakis, 2002). It covers the entire external surface and serves as an effective barrier against physical, chemical, and biological insults (Madison, 2003). In addition, skin is involved in thermoregulation and in prevention of excess water loss (Madison, 2003).

Different layers of the human skin include: epidermis, dermis, and hypodermis (Wysocki, 1999).

The most superficial epidermis is mainly composed of keratinocytes but also contains other cell populations, such as dendritic cells, melanocytes, Langerhans cells, and Merkel cells (Boulais and Misery, 2008). According to keratinocyte morphology and differentiation the epidermis can be divided from the deepest to the most superficial layer in: stratum basale, stratum spinosum, stratum granulosum, and stratum corneum (Simpson et al., 2011, Snell, 1965) (Fig. 1).

Mitotically active cells in the stratum basale give rise to cells to the outer epidermal layers. Keratinocyte differentiation occurs as cells migrate to the surface of the skin which takes at least 28 days in human skin (Abdo et al., 2020, Usui et al., 2008).

At the level of the basement membrane the epidermis connects to the underlying dermis. It is mostly composed of dense connective tissue that is divided into (i) the papillary layer which projects into the stratum basale of the epidermis and (ii) the reticular layer. The papillary dermis compromises a higher density of cells, a higher content of proteoglycans, and a weaker alignment of collagen fibers as compared to the reticular dermis (Meigel et al., 1977, Mine et al., 2008, Rippa et al., 2019, Smith and Melrose, 2015). The most prevalent cell type in the dermis are fibroblasts (Thulabandu et al., 2018). They are derived from the mesenchyme and play a pivotal role in the secretion of components of the extracellular matrix (ECM) (Tracy et al., 2016).

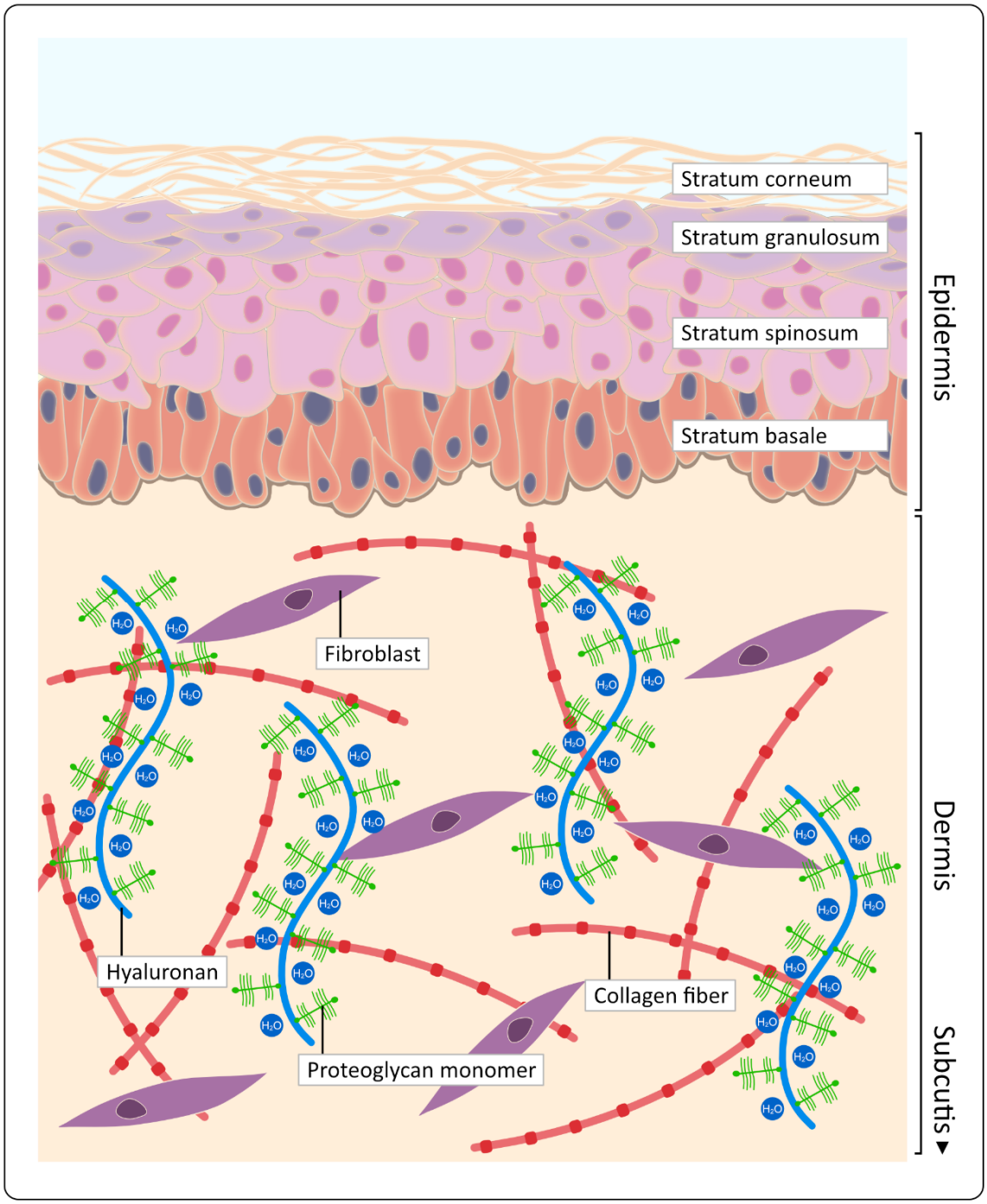

Fig. 1 Anatomy of human skin. Schematic illustration of distinct dermal components reflecting the complexity of their functions as a protective barrier. Human skin with a thickness of >100 µm consists of the epidermis, the dermis, and the subcutis. The epidermis is mainly composed of epidermal keratinocytes and can be divided into the stratum basale, the stratum spinosum, the stratum granulosum and the stratum corneum as the outermost barrier of the skin. Within the dermis, dermal fibroblasts produce and organize components of the extracellular matrix (ECM), e.g., collagen fibers and hyaluronan with proteoglycan monomers binding water molecules (H_2O). Modified after: Gerber et al., 2014, Nestle et al., 2009, Rock et al., 2012

1.2 Extracellular matrix

There are two main types of macromolecules which constitute the matrix: (i) proteoglycans (PGs) and (ii) fibrous proteins like collagens, elastins, fibronectins, and laminins (Iozzo et al., 2009). Whereas the fiber-forming molecules provide structure to the ECM by creating a complex three-dimensional framework, the nonfiber-forming structural molecules fill the extracellular interstitium forming a hydrated gel which functions as a charged, dynamic, and osmotically active space (Tracy et al., 2016). PGs are composed of glycosaminoglycan (GAG) chains which are covalently linked to a specific core protein – with the exception of hyaluronan (HA). GAGs are linear polysaccharide chains composed of repeating disaccharide units consisting of an amino sugar (*N*-acetylglucosamine (GlcNAc) or *N*-acetylgalactosamine (GalNAc)) and an uronic acid (glucuronic acid (GlcA)) that can be further divided into sulfated (chondroitin sulfate, heparan sulfate, and keratan sulfate) and non-sulfated HA (Frantz et al., 2010).
The ECM is a highly dynamic structure that undergoes constant remodeling to control tissue homeostasis. It interacts with epithelial cells to regulate diverse functions including proliferation, migration, and differentiation (Bonnans et al., 2014). Disturbances in the balance creates altered tissue architecture which impacts tissue function. Due to their ability to modify cellular properties, ECM components have become attractive targets for the emerging clinical use of bioactive wound dressing, engineered tissues, and topical wound treatments (Tracy et al., 2016).

1.3 Hyaluronan (HA)

HA consists of a linear polymer of repeating disaccharide units of [3)-β-D-*N*-acetylglucosamine (GlcNAc)-β(1,4)-D-glucuronic acid (GlcA)-β(1] (Kobayashi et al., 2020) (Fig. 2). Unlike other GAGs, HA does not contain any sulfate and is not covalently linked to a protein core, but it may form non-covalently linked complexes with other PGs (i.e., versican, aggrecan) creating a hydrated and charged domain.

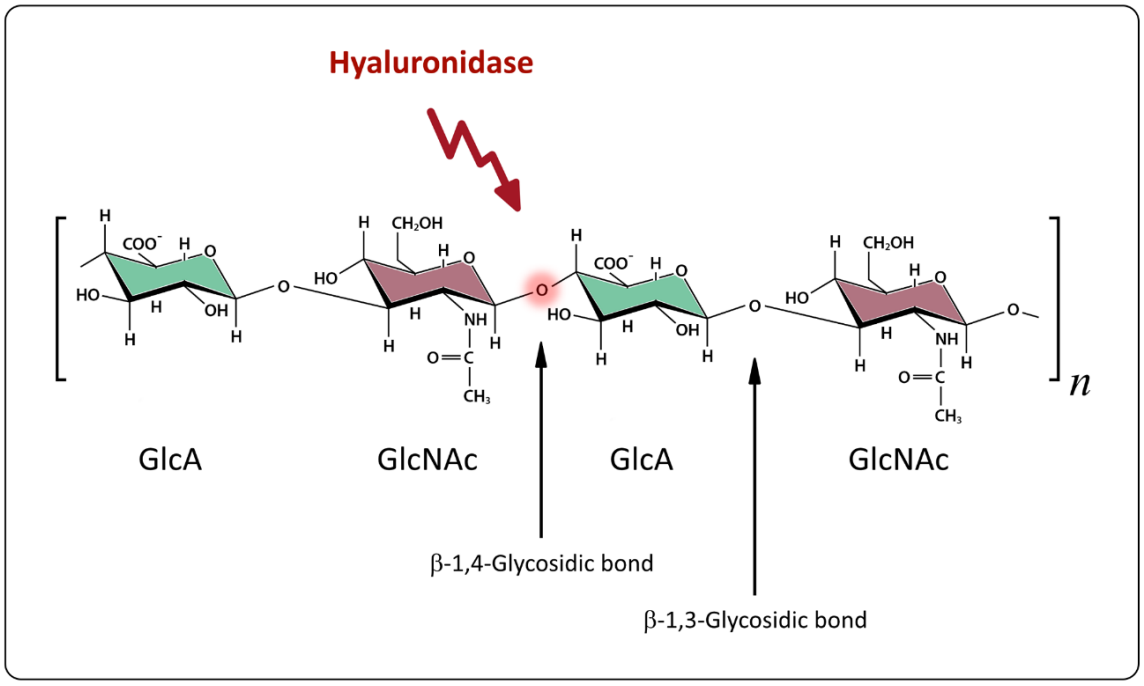

Fig. 2 Repeating disaccharide units of hyaluronan in human skin. Secondary chemical structure of negatively charged hyaluronan (HA) composed of n-repeating disaccharide units of glucuronic acid (GlcA) and *N*-acetylglucosamine (GlcNAc) with β-1,4- and β-1,3-glycosidic bonds. Hyaluronidase cleaves the bonds between GlcNAc and GlcA. Modified after: de Oliveira et al., 2016, Weber et al., 2019

Under physiological conditions, a typical polymer consists of 2,000 – 25,000 disaccharides (molecular mass 10^6 – 10^7 daltons (Da) with polymer lengths of 2 – 25 μm) (Toole, 2004). The total amount of HA in the human body is about 15 g for a 70 kg adolescent and has a high turnover of about 5 g per day which is precisely regulated through enzymatic synthesis and/or degradation (Volpi et al., 2009). HA is most abundant in the skin (approximately 50%) but can also be found in the vitreous of the eye, the umbilical cord, and synovial fluid (Fallacara et al., 2018). In the skin HA is present in both the dermal connective tissue and the intercellular space of epidermis with exception of the upper granular layer and the stratum corneum (Juhlin, 1997, Tammi et al., 1994). Due to its excellent water binding capacity and viscoelastic properties, which are attributed to a high density of negative chain charges from carboxyl groups HA is highly effective in skin hydration even at low concentrations (Laurent, 1989).

Besides providing structural framework in the ECM, HA has a wide variety of different functions which not only depend on chain length and concentration (Tavianatou et al., 2019), but also on the interaction with various HA-binding

proteins such as hyaladherins including aggrecan, neurocan, and versican. In addition, HA interacts with cell-surface receptors such as cluster determinant 44 (CD44) and the receptor for hyaluronic-acid-mediated motility (RHAMM) either direct or by activating other receptors (Girish and Kemparaju, 2007, Knudson and Knudson, 1993, Turley et al., 2002). Thus, HA plays fundamental roles in regulating morphogenesis, migration, proliferation, and wound healing (Laurent and Fraser, 1992). In contrast, dysregulation of HA metabolism can result in altered production of HA and is associated with inflammation, malignant transformation, and metastasis (Adamia et al., 2005, Adamia et al., 2013, Fallacara et al., 2018, Kobayashi et al., 2020).

1.4 Biological functions of hyaluronan polymers

Biological functions of HA can differ depending on chain length and molecular mass (Girish and Kemparaju, 2007, Toole, 2004). Fragment size of HA can vary from high molecular weight HA (HMW-HA; >4 × 10^5 Da) and medium molecular weight HA (MMW-HA; 5 × 10^4 – 4 × 10^5 Da) to low molecular weight HA (LMW-HA; <5 × 10^4 Da) (Buhren et al., 2016, Snetkov et al., 2020). Interestingly, HMW-HA and LMW-HA can exhibit completely opposite effects and can provoke different biological responses. Whereas HMW-HA can be involved in tissue homeostasis and promotes anti-inflammatory, anti-proliferative, and anti-angiogenic effects, the smaller HA fragments can lead to angiogenesis, cell proliferation, invasion, and inflammation (Bohaumilitzky et al., 2017, Stern et al., 2006, Tammi et al., 2002, Tavianatou et al., 2019, Weigel and Baggenstoss, 2017, Yang et al., 2012). Fragmentation of HMW-HA can result in two different ways: either mediated by enzymatic cleavage via exo-β-glycosidases and hyaluronidases (HYAL) or conducted non-enzymatically by reactive oxygen species (ROS) generated during inflammatory responses (Soltes et al., 2006, Weigel and DeAngelis, 2007). Indeed, increase in HA fragments might also be the result of HA synthases (HAS) when regulated to synthesize very small HA and thus producing smaller HA chains directly (Bracke et al., 2010, Lee-Sayer et al., 2015).

1.5 Hyaluronan biosynthesis

At the inner face of the plasma membrane HA is synthesized as a free linear polymer by specific enzymes (HA synthases; HAS) (Itano et al., 1999, Weigel et al., 1997). Three distinct highly conserved genes located on separated chromosomes encoding mammalian HAS have been cloned: HAS1 on human chromosome 19q13.4, HAS2 on human chromosome 8q24.12, and HAS3 on human chromosome 16q22.1 (Spicer et al., 1997). HAS isoforms exhibit distinct enzymatic properties in terms of activity and function which is regulated dynamically at transcriptional, post-transcriptional and post-translational levels (Heldin et al., 2019, Itano et al., 1999). Differential expression patterns of HA isoforms are cell-specific as they vary in different tissues and during different embryonic developmental stages and can be controlled by growth factors, cytokines and other proteins (Fallacara et al., 2018, Itano and Kimata, 2002). Of note, as biological and physiological roles of HA markedly depend on its size (Cyphert et al., 2015) each HAS can synthesize HA chains of various lengths (Weigel et al., 1997). *In vitro* analyzes revealed that HAS1 is the least active isoenzyme produces HA with an average molecular mass ranging from 2×10^5 to $\sim 2 \times 10^6$ Da (Itano and Kimata, 2002, Itano et al., 1999). HAS2 which represents the main HAS in normal adult cells is more active compared to HAS1 and synthesizes HA chains greater than 2×10^6 Da (Fallacara et al., 2018, Vigetti et al., 2014). HAS3 is the most active isoenzyme and produces HA of lower molecular weight size lower than 3×10^5 Da (Fallacara et al., 2018, Girish and Kemparaju, 2007, Papakonstantinou et al., 2012). As catalytic sites of HAS are located at the inner surface of the plasma membrane, the synthesized growing HA chains are extruded onto the cell surface in the plasma membrane via HAS protein complexes (Fallacara et al., 2018, Itano and Kimata, 2002, Weigel et al., 1997).

1.6 Hyaluronidase (HYAL)

Regulation of HA synthesis and degradation is fundamental for skin homeostasis. HYALs are endoglucosaminidases randomly cleaving the β-N-acetyl-d-glucosaminidic linkages (β-1,4 glycosidic bonds) of HA chains. Although they are

capable to hydrolyse chondroitin sulfate and chondroitin, they predominantly target HA (Fallacara et al., 2018, Stern and Jedrzejas, 2006). In humans, six gene sequences for HYAL genes have been recognized so far: gene sequences encoding for HYAL1, HYAL2, and HYAL3 which are clustered on chromosome 3p21.3 as well as gene sequences for HYAL4, sperm adhesion molecule 1 (SPAM1), and PHYAL1, a pseudogene, located on chromosome 7p31.3 (Csoka et al., 2001). In humans both HYAL1 and HYAL2 are the predominant isoforms to degrade HA and are highly expressed in somatic tissues (Csoka et al., 2001). Although similar in structure, they produce different reaction products. HYAL1 can use HA of any size as a substrate and degrades HA into small fragments of one to six disaccharides (Bohaumilitzky et al., 2017, Girish and Kemparaju, 2007, Tavianatou et al., 2019). HYAL2 hydrolyses specifically HMW-HA into LMW-HA, thereby creating HA fragments of approximately 20 kDa which can be further degraded to smaller oligomers (Papakonstantinou et al., 2012, Stern, 2004). Apart from specific enzymatic degradation by HYALs, HA can also be fragmented by ROS and nitrogen species which are predominantly produced during inflammatory responses, ischemia, and malignancies (Fallacara et al., 2018, Soltes et al., 2006, Tavianatou et al., 2019).

1.7 Biomedical application of HA and HYAL

Due to its hygroscopic and highly viscoelastic nature, HA and HA-based products have gained popularity as major parts of pharmaceutical and biomedical components. Following large scale industrial preparation mostly via bacterial fermentation by *Streptococci* strains, HA has been implemented in a variety of biomaterial in clinical settings (Sze et al., 2016) such as skin tissue engineering in terms of wound dressing (Aya and Stern, 2014) but also soft tissue augmentation (Tezel and Fredrickson, 2008), viscosupplementation in osteoarthritis (Moreland, 2003), and opthalmological surgery (Neumayer et al., 2008). In order to overcome rapid *in vivo* degradation of native HA, a number of chemical modification strategies including conjugation and crosslinking of HA have been developed recently to produce more insoluble HA polymers with improved customized activities (Fallacara et al., 2018, Knopf-Marques et al., 2016). Degradability studies show that the concentration and the degree of

crosslinking of native HA can affect sensitivity to enzymatic degradation by HYAL (Buhren et al., 2018). As an endoglycosidase, HYAL cleaves HA thereby increasing membrane permeability, reducing viscosity, and rendering tissues more permeable to injected fluids which is characterized as a spreading effect (Buhren et al., 2016, Girish and Kemparaju, 2007). Thus, currently HYAL is frequently used to accelerate subcutaneous drug adsorption and dispersion (Kallio et al., 2000), for hypodermoclysis (Constans et al., 1991), management of extravasation injuries (Bellin et al., 2002), and dissolution of misplaced HA-based fillers (Bailey et al., 2014, Weber et al., 2019). Different commercially available formulations of HYAL that have been used in several medical fields include agents derived from purified bovine testis (Hylase Dessau®, Riemser Pharma GmbH, Greifswald, Germany), from purified ovine testis (Vitrase®, ISTA Pharmaceuticals (Bausch & Lomb), Bridgewater, NJ), and human recombinant agents (Hylenex®, Halozyme, San Diego, CA) (Lee et al., 2010).

1.8 Institutional review board statement

The study was reviewed and approved by the institutional review board, the "Ethikkommission an der Medizinischen Fakultät der Heinrich-Heine-Universität Düsseldorf" (study numbers 2882 & 6058R).

1.9 Aim of the thesis

The extracellular matrix (ECM) of the skin comprises a three-dimensional network which is composed of an array of macromolecules organized in a cell-specific manner providing tensile strength but also playing a role in the regulation of a wide variety of cellular mechanisms including proliferation, adhesion, migration, and gene regulation. One significant but also abundant component of the ECM is HA. Due to its unique hydrophilic nature, it has the capacity to bind and retain great amounts of water thereby influencing physicochemical properties and cell biological functions of tissues. Degradation of HA can occur through free chemical radicals and enzymatically by different hyaluronidases (HYAL1 – 2) leading to smaller fragments of different sizes, which are then further degraded. Interestingly, biological functions of HA are related directly to its fragment size.

Therefore, the synthesis of individual-sized HA fragments but also the size-dependent degradation of high molecular weight HA by HYAL is critically involved in the regulation of the ECM. To date, limited information is available regarding the mechanisms of HA catabolism and HYAL-HA interactions at the cellular and molecular levels in the skin.

In this thesis the following points were addressed:

1. Comprehensive genome-wide Affymetrix GeneChip® expression analyses of HA and HYAL application in structural cells of the skin (human dermal fibroblasts (NHDF), human epidermal keratinocytes (HEK)).
2. Dose-dependent effects on the biosynthesis of HA following HA and HYAL application in NHDF and HEK.
3. Time-kinetic effects on the biosynthesis of HA following HA and HYAL application in NHDF and HEK.
4. Role of HA and HYAL on the healing of artificial wounds *in vitro.*

2. Published paper

Buhren *et al. Eur J Med Res* (2020) 25:60
https://doi.org/10.1186/s40001-020-00460-z

European Journal of Medical Research

RESEARCH Open Access

Dose- and time-dependent effects of hyaluronidase on structural cells and the extracellular matrix of the skin

Bettina Alexandra Buhren[1], Holger Schrumpf[1], Katharina Gorges[2], Oliver Reiners[2], Edwin Bölke[3], Jens W. Fischer[2], Bernhard Homey[1] and Peter Arne Gerber[1,4*]

Abstract

Introduction: Hyaluronic acid (hyaluronan; HA) is an essential component of the extracellular matrix (ECM) of the skin. The HA-degrading enzyme hyaluronidase (HYAL) is critically involved in the HA-metabolism. Yet, only little information is available regarding the skin's HA–HYAL interactions on the molecular and cellular levels.

Objective: To analyze the dose- and time-dependent molecular and cellular effects of HYAL on structural cells and the HA-metabolism in the skin.

Materials and methods: Chip-based, genome-wide expression analyses (Affymetrix® GeneChip PrimeView™ Human Gene Expression Array), quantitative real-time PCR analyses, enzyme-linked immunosorbent assay (ELISA), immunohistochemistry (DAB), and in vitro wound healing assays were performed to assess dose-dependent and time-kinetic effects of HA and HYAL (bovine hyaluronidase, Hylase "Dessau") on normal human dermal fibroblasts (NHDF), primary human keratinocytes in vitro and human skin samples ex vivo.

Results: Genome-wide expression analyses revealed an upregulation of HA synthases (HAS) up to 1.8-fold change in HA- and HYAL-treated NHDF. HA and HYAL significantly accelerated wound closure in an in vitro model for cutaneous wound healing. HYAL induced HAS1 and HAS2 mRNA gene expression in NHDF. Interestingly, low concentrations of HYAL (0.015 U/ml) resulted in a significantly higher induction of HAS compared to moderate (0.15 and 1.5 U/ml) and high concentrations (15 U/ml) of HYAL. This observation corresponded to increased concentrations of HA measured by ELISA in conditioned supernatants of HYAL-treated NHDF with the highest concentrations observed for 0.015 U/ml of HYAL. Finally, immunohistochemical analysis of human skin samples incubated with HYAL for up to 48 h ex vivo demonstrated that low concentrations of HYAL (0.015 U/ml) led to a pronounced accumulation of HA, whereas high concentrations of HYAL (15 U/ml) reduced dermal HA-levels.

Conclusion: HYAL is a bioactive enzyme that exerts multiple effects on the HA-metabolism as well as on the structural cells of the skin. Our results indicate that HYAL promotes wound healing and exerts a dose-dependent induction of HA-synthesis in structural cells of the skin. Herein, interestingly the most significant induction of HAS and HA were observed for the lowest concentration of HYAL.

Keywords: Skin, Dermatology, Metabolism, Enzymes, Cell

*Correspondence: prof.gerber@dermatologie-am-luegplatz.de
[4] Dermatologie am Luegplatz, Duesseldorf, Germany
Full list of author information is available at the end of the article

Introduction

The extracellular matrix (ECM) of the skin is a complex network of macromolecules, and plays an important role in the regulation of numerous cellular mechanisms such as proliferation, adhesion, migration, and gene regulation

in addition to their mechanically stabilizing function [5]. A functionally and quantitatively important component of dermal ECM is hyaluronic acid (hyaluronan; HA) [26]. Approximately half of all HA in the body is contained within skin tissue. Due to its hydrophilic properties, HA binds high volumes of water which in turn determines the physical properties of tissues (e.g., the viscoelasticity of the skin) [31]. In contrast to other dermal glycosaminoglycans, the biosynthesis of HA does not take place in the Golgi apparatus, but on the inside of the cell membrane by localized HA synthases (HAS1, HAS2 and HAS3) [11]. The different HAS isoforms produce HA which differs primarily in the polymer size. HAS1 and HAS3 synthesize HA polymers in the order of 2×10^5 to 2×10^6 Da, while HAS2 forms HA polymers $> 2 \times 10^6$ Da [59]. The half-life of HA is organ-dependent and is approximately 24 h in the skin. The degradation of HA is mediated via free chemical radicals and different hyaluronidases (HYAL1 and HYAL2) first into smaller fragments of different sizes, which are then further degraded [51].

Depending on the fragment size, degradation products also have differing biological properties and may, for example induce neovascularization resulting in a proinflammatory response. The expression of different sized HA fragments and also the degradation of HA to HA fragments of different sizes are thus critically important in the regulation of the ECM [27]. Hence, in addition to its importance as a structural molecule, HA is also considered a functional molecule, depending upon its molecular size [14, 55].

In ophthalmological and surgical applications, HYAL is primarily employed as a so-called spreading factor for cutaneous infiltration, as the addition of HYAL to infiltrating local anesthetics accelerates anesthetic diffusion and expansion of the anesthetized area [40, 58, 60]. In addition to its use in local anesthesia, HYAL is used to manage complications following aesthetic injections of HA-fillers. In aesthetic medicine the injection of HA-based fillers for soft tissue augmentation, deep skin hydration or facial contouring has become increasingly popular over the past decades. Besides overcorrections potential complications of aesthetic HA-fillers include edema, infections, or even skin necrosis or visual complications [6, 22, 25, 58]. As HYAL has the potency to effectively degrade HA-based fillers, the off-label use of HYAL is considered as the gold standard for the management of complications of HA fillers [6]. To date, little information is available regarding the mechanisms of HA catabolism and HYAL–HA interactions at the cellular and molecular levels in the skin. We therefore systematically assessed the molecular and cellular effects of HA and HYAL (Hylase® "Dessau") on the gene regulation in structural skin cells and evaluated the role of HA and HYAL on the healing of artificial wounds in vitro.

Materials and methods

Reagents

The hyaluronan (HA) Juvederm Ultra 3 (Allergan, Dublin, Ireland) has been widely used as an injectable filler in aesthetics dermatology. Its main indication is filling of folds and correction of soft tissue loss due to disease or age [19]. Juvederm Ultra 3 is made of cross-linked HA in a monophasic state and contains HA in a mixture of high-molecular-weight (HMW) polymers of 491 kDa (38%) and low-molecular-weight (LMW) polymers of 134 kDa (62%) [17]. We decided to use the dose of 1 mg/ml as this concentration turned out to be optimal in our preliminary experiments, especially with regard to handling (viscosity, etc.). In addition, this specific concentration has been widely used and published in previous studies [10, 24].

For the hyaluronidase (HYAL) Hylase "Dessau" (Riemser, Greifswald, Germany), we decided to use tenfold serial dilutions allowing us to compare a wide range of doses. This is a common method for such dose-range findings, the dose-by-factor approach [39, 48]. The stock concentration of Hylase "Dessau" was 150 U/ml. This value was divided multiple times by 10 in order to obtain the following concentrations in "International Units": 15 U/ml, 1.5 U/ml, 0.15 U/ml and 0.015 U/ml.

Cell culture

All research involving human samples was approved by the Medical Faculty of the University of Duesseldorf. Written informed consent was obtained from each participant.

The commercially available normal human dermal fibroblasts (NHDF) were isolated from the dermis of juvenile foreskin (PromoCell, Heidelberg, Germany) and handled according to the manufacturer's instructions. Briefly, for experimental setup NHDF were cultured in 6-well plates at 37 °C in 5% CO_2 in cell-specific medium Quantum 333 (PAA, Pasching, Austria) supplemented with 2 mM L-glutamate, 100 U/ml penicillin, and 100 µg/ml streptomycin. When the cells reached approximately 80% of confluency (80% of surface of flask covered by cell monolayer) they were used for experiments.

The primary human keratinocytes were used as described elsewhere [33]. In more detail, primary human keratinocytes were isolated from non-sun-exposed adult skin (age ranged from 35 to 60 years; mean age was 47). After fat and loose fascia were trimmed, skin fragments were placed into 50 ml tubes at 4 °C overnight for dispase digestion (1.5 U/ml; GIBCO, Invitrogen, Carlsbad, USA). The epidermal pieces were transferred to another tube containing 2 ml 0.05% trypsin/EDTA solution (Merck, Darmstadt, Germany) and were incubated for about 30 min. Following neutralization, the

cell suspension of epidermal cells was filtered and finally released into keratinocyte-SFM medium (ThermoFisher, Waltham, MA), supplemented with recombinant EGF, pituitary extract, 2 mM L-glutamate, 100 U/ml penicillin, and 100 µg/ml streptomycin. Cells were then cultured at 37 °C and 5% CO_2 in 6-well plates until cells reached approximately 80% of confluency or cryopreserved until further use.

The number of different individual donors was $n \leq 6$ for keratinocytes. The age of donors ranged from 35 to 60 years, the mean age was 47. For fibroblasts, the number of different independent experiments was $n = 4$.

Primary cells were treated with 1 mg/ml HA Juvederm Ultra 3 and/or HYAL Hylase "Dessau" for different incubation time points (0 h, 4 h, 12 h, 24 h) and different enzyme doses (15 U/ml, 1.5 U/ml, 0.15 U/ml, 0.015 U/ml).

For investigation of the Affymetrix®-based genome-wide expression analysis, cells were treated with 1 mg/ml Juvederm Ultra 3 HA and/or 1.5 U/ml HYAL for 24 h.

RNA extraction

RNA from primary human keratinocytes and NHDF was isolated for expression analyzes using RNeasy Mini Kit (Qiagen, Hilden, Germany) according to the manufacturer's protocol. The yield of RNA was determined using a NanoDrop™ 2000c photometer (ThermoFisher, Waltham, MA). A value between 1.8 and 2.1 for the OD 260/280 [optical density (OD) ratio at a wavelength of 260/280 nm] indicated that the extracted RNA contained no interfering proteins, salts or other contaminants. The quality of RNA obtained was subsequently checked bioanalytically (Agilent® Bioanalyzer assay RNA 6000 Pico Chip™, Santa Clara, CA).

Microarray hybridization

For the assessment of gene regulation by means of Affymetrix® chip-based, genome-wide expression analysis the hybridization of purified and bioanalytically immaculate RNA [RNA Integrity Number (RIN) > 9] from NHDF was carried out according to the manufacturer's instructions, followed by statistical analysis. Background adjustment, signal normalization, and summarization were performed using the Robust Multi-array Average (RMA) algorithm in ArrayAssist™ software (Iobion Labs, La Jolla, CA). Raw data, filtered by expression (20th to 100th percentile), were output as fold change ($\geq \pm 1.5$). Untreated (medium only) NHDF were used as controls.

Quantitative real-time PCR analysis

Quantitative real-time PCR analysis was performed as described by Homey and colleagues [23]. RNA from both primary human keratinocytes and NHDF was treated with DNase I (Roche, Basel, Switzerland) and reverse transcribed with Oligo(dT)12–18 (ThermoFisher, Waltham, MA) and random hexamer primers (Promega, Madison, WI) using standard protocols. cDNA was analyzed for the expression of human HAS1, HAS2 and HAS3 genes using a QuantStudio™ 6 Flex Real-Time PCR System (ThermoFisher, Waltham, MA). cDNA was amplified in the presence of SYBR™ Green master mix (ThermoFisher, Waltham, MA), gene-specific forward and reverse primers, and water. Primers were obtained from Eurofins Genomics (Ebersberg): HAS1 forward 5′-TCG GAGATTCGGTGGACTA-3′, reverse 5′-AGGAGTCCA GAGGGTTAAGGA-3′, HAS2 forward 5′-GTGGAT TATGTACAGGTTTGTGA-3′, reverse 5′-TCCAACCAT GGGATCTTCTT-3′, HAS3 forward 5′-CGATTCGGT GGACTACATCC-3′, reverse 5′-CCTACTTGGGGA TCCTCCTC-3′. Target gene expression was normalized to the expression of 18S rRNA.

Cutaneous wound healing assay

Tissue regeneration is quite a complex process that consists of a sequence of events including inflammation, proliferation, and migration of different cells like fibroblasts [4]. There are a number of human in vitro models available which include different levels of complexity. In line with the 3Rs (reduction, refinement and replacement of test animals), we investigated cell mobility during wound healing in a scratch wound healing assay [38]. In our analyses this assay was established on a monolayer of normal dermal human fibroblasts to study random fibroblast migration towards different treatment conditions.

Therefore, NHDF were cultured in 12-well plates until 95% confluency. Cells were treated as previously described. In addition, NHDF treated with medium-sized HA (Hyaluronan (Medium MW), R&D Systems, Minneapolis, USA) with a fragment size from 75 to 350 kDa were used. The monolayer of cells was scratched across each well using a fine pipette tip in order to create a cell-free area. The condition of scratches was detected from time point 0 using a digital time lapse video system (Zeiss® Axiovert™ 200M and AxioVision™ software 4.7, Oberkochen, Germany) over a period of 50 h. The evaluation of end-point assays was carried out by comparing the wound closure of the control with the wound healing response of cells treated with HA and/or HYAL using the program TScratch (CSElab, Zurich, Switzerland).

Enzyme-linked immunosorbent assay (ELISA)

HA concentrations in the supernatants of HA- and/or HYAL-stimulated primary human keratinocytes and NHDF were measured using an enzyme-linked immunosorbent assay (DuoSet® ELISA, R&D Systems, Minneapolis, USA).

This assay was performed according to the manufacturer's instructions and is able to detect the low-molecular weight (15–40 kDa), medium molecular weight (75–350 kDa), and high molecular weight (>950 kDa) forms of hyaluronan.

Briefly, monoclonal capture antibody was incubated overnight in the wells of an immunosorbent 96-well plate. After blocking with reagent diluents (1% BSA in PBS) for 1 h at room temperature, wells were aspirated and rinsed with washing buffer (0.05% Tween® 20 in PBS). Following another aspiration and washing step, biotinylated detection antibody was incubated for 2 h. After next aspiration and washing step, streptavidin-HRP was incubated for 20 min. Following a final aspiration and washing step, substrate solution was incubated for 20 min. Finally, stop solution was added. Optical densities were measured at 450 nm by using a microplate reader. Sample concentrations were calculated against standard curves.

Skin organ cultures

Human skin bunch biopsies, isolated from non-sun-exposed adult skin (age ranged from 35 to 60 years), were obtained from individuals following elective surgery with full ethical approval and informed consent. The skin samples were processed to remove the underlying fat and connective tissue. Ex vivo skin samples were cultured at the air–liquid interface with the epidermal side up 48 h in keratinocyte-SFM (ThermoFisher, Waltham, MA) supplemented with recombinant EGF and stimulated for 24 h at 37 °C as mentioned above, followed by washings three times for 5 min with phosphate-buffered saline (PBS). Thereafter ex vivo skin samples were fixed with 10% buffered formalin, and embedded in paraffin wax before performing 10-µm cross skin sections.

Immunohistochemistry (DAB) on paraffin-mounted normal skin tissue slides

Heat-fixed paraffin-mounted normal skin slides were deparaffinized three times with Roticlear® I, II, III (Roth AG, Arlesheim, Switzerland) for 15 min per treatment, then hydration once each to 100%, 95%, and 70% ethanol for 2 min, followed by washings with PBS. Slides were subjected to immunohistochemistry by using a DAB staining kit (Vector Laboratories, Burlingame, CA). Briefly, the slides were blocked for 20 min using an avidin/biotin blocking kit (Vector Laboratories, Burlingame, CA), followed by washing with PBS. Then, slides were blocked for 30 min with 1% BSA/10% FCS in TBS followed by incubation with a biotinylated HA binding protein (Merck Chemicals GmbH, Darmstadt, Germany) (1:200) in 1% BSA overnight at 4 °C. After washings with PBS and blocking with 3% H_2O_2 in between, slides were then rinsed with PBS and incubated with secondary antibody for 1 h at room temperature. The slides were washed again and developed with 3,3′-diaminobenzidine (DAB) as substrate according to the manufacturer's instructions. Subsequently, a nuclear staining with hemalum was performed. The slides were mounted with Roti®-Mount (Roth AG, Arlesheim, Switzerland). For quantification of DAB staining, slides were photographed by a Zeiss® Axiovert™ 200M microscope and AxioVision™ software 4.7 (Oberkochen, Germany). Next, DAB staining was analyzed by ImageJ software (BioVoxxel Fiji ImageJ 1.49 m). Values were normalized and represented as positive staining per area in relative units.

Statistical analysis

Data were expressed at mean ± standard error of the mean (SEM). Statistical significance was assessed by Student's *t*-test. *P*-values less than or equal to 0.05 were considered statistically significant ($^{*}p \leq 0.05$, $^{**}p \leq 0.01$, $^{***}p \leq 0.001$).

Results

HYAL and HA induce HAS expression in NHDF in vitro

Affymetrix® expression analyses were carried out to systematically investigate the effects of HA and HYAL in NHDF. Subsequently, in comprehensive bioinformatic analyses, gene lists containing the 50 most upregulated and most downregulated genes were generated (Additional file 1: Tables S1–S6). In NHDF HAS1 and HAS2, transcription level increased 1.2-fold after stimulation with HA. In contrast, HA stimulation decreased gene expression of HAS3 (Fig. 1a). Interestingly, in HYAL-treated NHDF transcription levels of all three HASs increased up to 1.8-fold changes (Fig. 1b).

HYAL and HA induce HAS in a time- and dose-dependent manner in vitro

To analyze time-kinetic and dose-dependent effects, NHDF and primary human keratinocytes were stimulated with HA and HYAL for different time periods (2 h, 4 h, 12 h and 24 h) as well as different concentrations (15 U/ml, 1.5 U/ml, 0.15 U/ml, 0.015 U/ml).

Stimulation with HA as well as HYAL (1.5 U/ml) for 24 h significantly increased gene expression of HAS2 in NHDF compared to medium controls (Fig. 2a, $p = 0.0090$; $p = 0.0319$). In addition, HYAL treatment for 2 h and 12 h significantly increased gene expression of HAS2 compared to respective medium controls (Fig. 2a, $p = 0.0012$; $p = 0.0038$) with no observed effect for HA. Co-stimulation of HA and HYAL (1.5 U/ml) had no impact on HA synthase gene expression compared to medium control (Fig. 2a, Additional file 1: Figure S1A, C). In contrast, HAS1 expression was significantly induced by HA after 2 h compared to medium controls (Additional file 1:

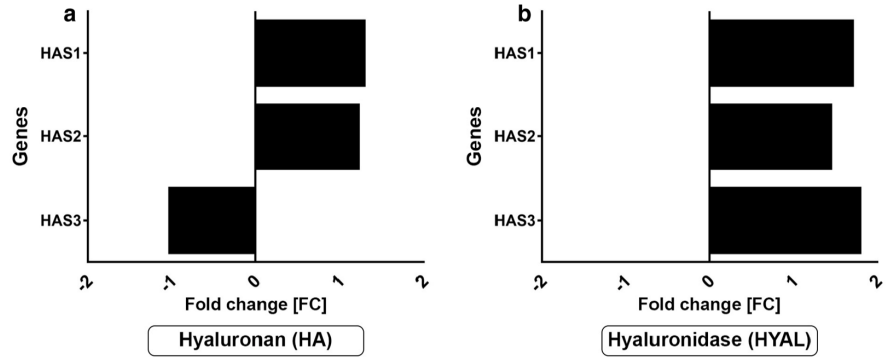

Fig. 1 Hyaluronan (HA) and hyaluronidase (HYAL) induce the mRNA expression of HA synthases. Affymetrix® GeneChip expression data ($n=1$) of **a** HA- and **b** HYAL-treated NHDF shown as fold changes [FC]

Figure S1A, $p=0.0401$). Incubation with HYAL (1.5 U/ml) increased gene expression of HAS1 at earlier time points (2 h, 4 h) (Additional file 1: Figure S1A, $p=0.0026$; $p=0.0246$). The gene expression profile of HAS3 demonstrated no significant differential regulation when NHDF were treated with HA and/or HYAL (Additional file 1: Figure S1C). In contrast, human epidermal keratinocytes (HEK) were less responsive to HA and HYAL with regard to HAS1 and HAS2 relative gene expression levels compared to NHDF (Additional file 1: Figure S2A–D). Expression of HAS1 was significantly downregulated at 24 h after stimulation with HA ($p=0.0062$), HYAL (1.5 U/ml) ($p=0.0021$) and co-stimulation of HA and HYAL ($p=0.0023$) as compared to medium control (Additional file 1: Figure S2A). At early time points (2 h, 4 h) co-stimulation with HA and HYAL showed significant downregulation of HAS3 (Additional file 1: Figure S2E, $p=0.0317$; $p=0.0032$).

Next, different doses of HYAL were tested in NHDF. Interestingly, HAS2 expression increased with decreasing concentrations of HYAL (Fig. 2b). Notably, the lowest tested concentration of HYAL (0.015 U/ml) demonstrated a highly significant induction of HAS2 expression compared to medium control (Fig. 2b, $p=0.0002$). Similarly, incubation with HYAL at its lowest concentration also induced gene expression of HAS1 (Additional file 1: Figure S1B, $p=0.0106$). Gene expression of HAS3 was not affected when NHDF were stimulated with different doses of HYAL (Additional file 1: Figure S1D). Varying doses of HYAL were then tested in primary human keratinocytes. In contrast, stimulation with HYAL significantly decreased expression of HAS1 (Additional file 1: Figure S2B) while HAS2 and HAS3 were not affected by varying doses of HYAL for 24 h (Additional file 1: Figure S2D, F).

HYAL induces HA production in NHDF but not in HEK in a time- and dose-dependent manner in vitro

To analyze soluble HA release, conditioned supernatants of time- and dose-dependent experiments (see above) in NHDF and primary human keratinocytes were analyzed by ELISA. HA secretion increased continuously over time in medium control (Fig. 2c, Additional file 1: Figure S1G). As expected, the addition of HA to primary cells resulted in a higher concentration of HA. Treatment with HYAL (1.5 U/ml) reduced HA concentration at 12 h ($p=0.0209$) and 24 h ($p<0.0001$) compared to medium controls in NHDF. Co-stimulation with HYAL and HA decreased HA-concentration over time compared to stimulation with HA only. Next, supernatants of cells stimulated with varying HYAL concentrations were analyzed. Interestingly, while the incubation with higher concentrations of HYAL (15 U/ml and 1.5 U/ml) showed significantly lower concentrations of HA (Fig. 2d, $p<0.0001$; $p<0.0001$), treatment with HYAL at lower concentrations (0.15 U/ml and 0.015 U/ml) significantly increased the concentration of HA when compared to medium controls in NHDF (Fig. 2d, $p=0.0286$; $p=0.0035$). Similar to NHDF, the concentration of HA in supernatants of keratinocytes also increased over time in medium-treated controls (Additional file 1: Figure S2G). The addition of HA increased HA-concentrations in supernatants, which was only marginally reduced in co-stimulated cells. Compared to medium controls, HA concentrations decreased in HYAL (1.5 U/ml) treated keratinocytes at all tested time points (2 h, 4 h, 12 h, 24 h). In contrast to NHDF, the stimulation with different doses of HYAL significantly reduced HA concentrations for tested doses (1.5 U/ml, 0.15 U/ml and 0.015 U/ml) compared to medium controls (Additional file 1: Figure S2H, $p=0.0001$, $p=0.0001$, $p=0.0005$).

(See figure on next page.)

Fig. 2 **a** HAS2 gene expression levels ($n=4$) in normal human dermal fibroblasts (NHDF) after stimulation with 1 mg/ml HA, 1.5 U/ml HYAL and HA + HYAL co-stimulation for 2 h, 4 h, 12 h and 24 h; **b** HAS2 gene expression levels of NHDF after stimulation with 15 U/ml, 1.5 U/ml, 0.15 U/ml and 0.015 U/ml HYAL for 24 h. **c**, **d** HA amount (ng/ml) measurement by means of ELISA ($n=4$) in supernatants of NHDF treated as described in **a** and **b**. **e**–**k** Show representative histological HA-stained sections of human skin samples treated with **e** control (CTRL) medium, **f** 1 mg/ml HA, **g** 15 U/ml HYAL, **h** 1.5 U/ml HYAL, **i** 0.15 U/ml HYAL and **j** 0.015 U/ml HYAL, scale bars = 50 µm. **k** Quantification of HA-positive staining measured in CTRL, HA and HYAL (15 U/ml, 1.5 U/ml, 0.15 U/ml and 0.015 U/ml) treated skin samples plotted as individual values of $n=4$, mean values are shown by the horizontal bar. Asterisks above columns indicate statistical significant differences compared to their respective medium controls, $^{*}p \leq 0.05$, $^{**}p \leq 0.01$, $^{***}p \leq 0.001$ (*t*-test, two-sided)

HYAL induces HA in full-thickness human skin samples in a time- and dose-dependent manner ex vivo

Full-thickness human skin samples were treated with HA as well as different doses of HYAL (15 U/ml, 1.5 U/ml, 0.15 U/ml, 0.015 U/ml) ex vivo. Following paraffin embedding and sectioning, skin sections were stained with a biotinylated HA-binding protein to visualize accumulation of HA in the skin by immunohistochemistry (Fig. 2e–j). Computer-assisted quantification of staining intensities showed an induction of HA in HA-treated samples as compared to medium controls (Fig. 2k). Of note, incubation with HYAL at the lowest concentration (0.015 U/ml) resulted in a significantly stronger staining intensity of HA as compared to medium controls (Fig. 2k, $p=0.0286$).

HA and HYAL promote wound healing in vitro

Finally, scratch assays were performed to analyze the effects of HA and HYAL on wound healing in vitro. A NHDF monolayer was used to asses wound healing which comprises fibroblast migration and proliferation. Therefore, monolayers of cells were scratched and thereafter stimulated with HA, medium-sized HA and HYAL. Wound closure of treated monolayers was compared to medium controls over 50 h. Stimulation with HA (Fig. 3c, d) and HYAL (Fig. 3g, h) resulted in significantly accelerated wound healing as compared to medium controls (Fig. 3a, b). At 24 h, 83% (HA: $p=0.0036$, HYAL: $p=0.0058$) of the scratch area was closed for HA and HYAL as compared to 60% of wound closure for medium-treated controls (Fig. 3i). No significant differences were found for medium-sized HA (Fig. 3e, f) as compared to medium controls (Fig. 3i).

Discussion

To date, the effects of HA and HYAL on structural cells of the skin have been poorly characterized. Here, we examined these effects by comprehensive genome-wide gene chip analyzes followed by qPCR validation and quantitative protein analyzes.

Comprehensive literature suggests a predominant role of fibroblasts in HA metabolisms. In previous studies, Röck et al. found that HA is synthesized and incorporated as a quantitative and functionally important component into the dermal ECM [47].

There are a variety of chemical signals known to stimulate HA synthesis in human fibroblasts such as cytokines, decreased pH, growth factors as well as enzymatic degradation of HA [20, 29, 30]. Underlying mechanisms remain unclear. In line with other findings, enzymatic degradation of HA but also HA itself was found to stimulate HA in an in vitro cell culture system. In ^{3}H-glucosamine labeling experiments Moczar and Robert found that treatment of human skin fibroblasts with bovine testicular hyaluronidase increased the amount of newly synthesized HA in the medium [37]. In line with these results, our results show that HYAL increased HA amounts in conditioned supernatants of NHDF as measured by ELISA.

Interestingly, increased HA amounts were found particular in supernatants of those cells which showed high gene expression of HAS2 but no other isoforms. In various studies the HAS isoform HAS2 has been suggested to be most important for HA synthesis. HAS2 is the only HAS gene which deletion causes a lethal phenotype: HAS2 knockout mice die at embryonic day (E) 9.5 due to a failure to form HA-rich organs [8]. This confirms the predominant role of HAS2 in the regulation of HA and reveals its important role for HA-metabolism. Moreover, HAS2 appeared to be the predominant isoform in skin fibroblasts, based on the results of the quantitative real-time RT-PCR [47]. In addition Averbeck et al. [2] found that HAS-1 and HAS-2 were much more highly expressed in fibroblasts than in HaCaT and human skin.

However, the increase of HA amount in the supernatants could either result from (i) increase in HA synthesis or (ii) clearing of membrane-bound HA, but also (iii) increase of HA degradation mediated by HYAL. Since HYAL activity was not investigated in our experiments, further studies are required to address this specific question.

In titration experiments we showed that HAS2 gene expression increased with decreasing concentrations of HYAL. Interestingly, HYAL at its lowest concentration (0.015 U/ml) led to the strongest induction of HAS2. Correspondingly, the amount of newly synthesized

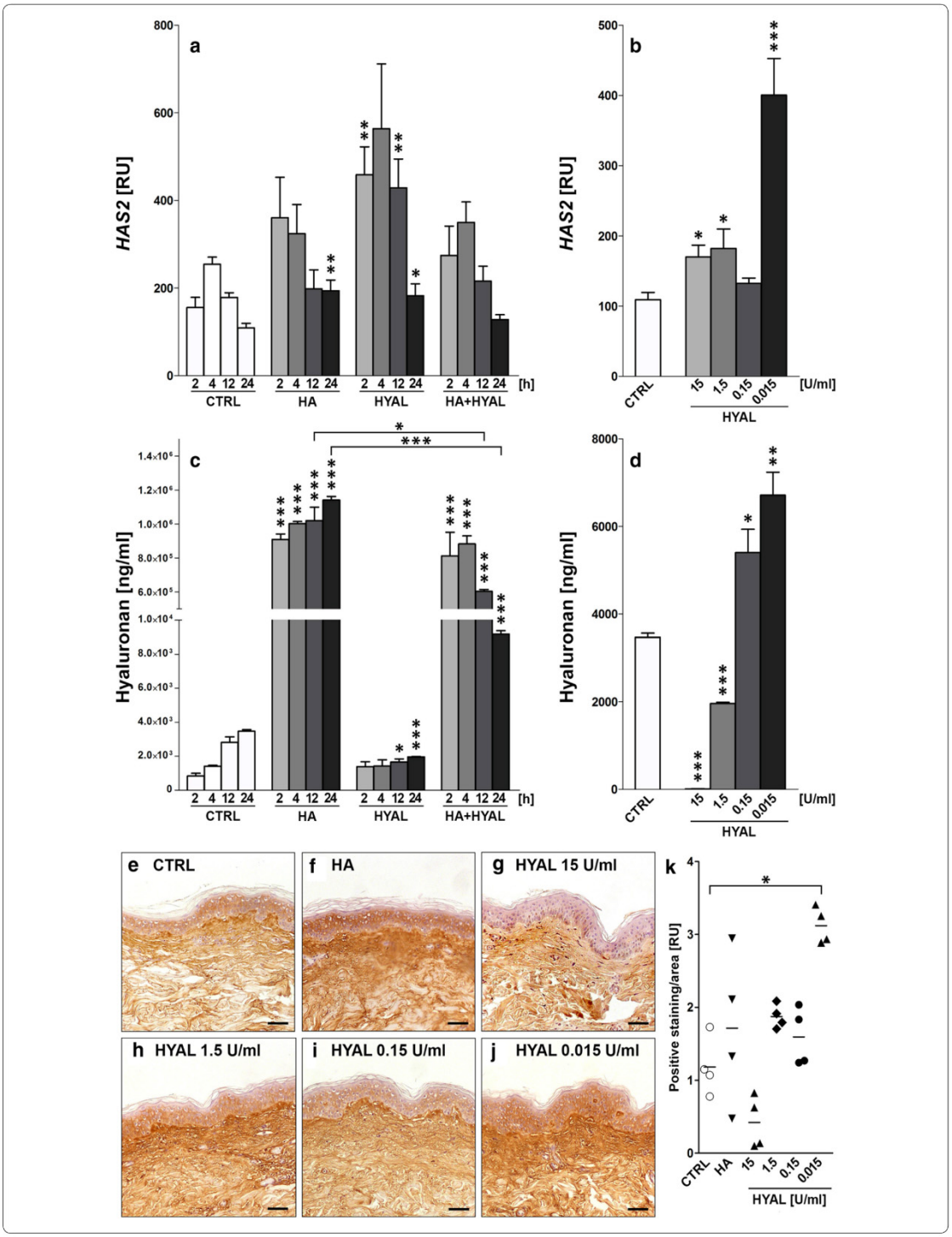
a
HAS2 [RU]
800
600
400
200
0
2 4 12 24 [h]
CTRL
HA
HYAL
HA+HYAL
b
HAS2 [RU]
500
400
300
200
100
0
CTRL
15 1.5 0.15 0.015 [U/ml]
HYAL
c
Hyaluronan [ng/ml]
1.4×10⁶
1.2×10⁶
1.0×10⁶
8.0×10⁵
6.0×10⁵
1.0×10⁴
8.0×10³
6.0×10³
4.0×10³
2.0×10³
0
2 4 12 24 [h]
CTRL
HA
HYAL
HA+HYAL
d
Hyaluronan [ng/ml]
8000
6000
4000
2000
0
CTRL
15 1.5 0.15 0.015 [U/ml]
HYAL
e CTRL
f HA
g HYAL 15 U/ml
h HYAL 1.5 U/ml
i HYAL 0.15 U/ml
j HYAL 0.015 U/ml
k
Positive staining/area [RU]
4
3
2
1
0
CTRL HA 15 1.5 0.15 0.015
HYAL [U/ml]

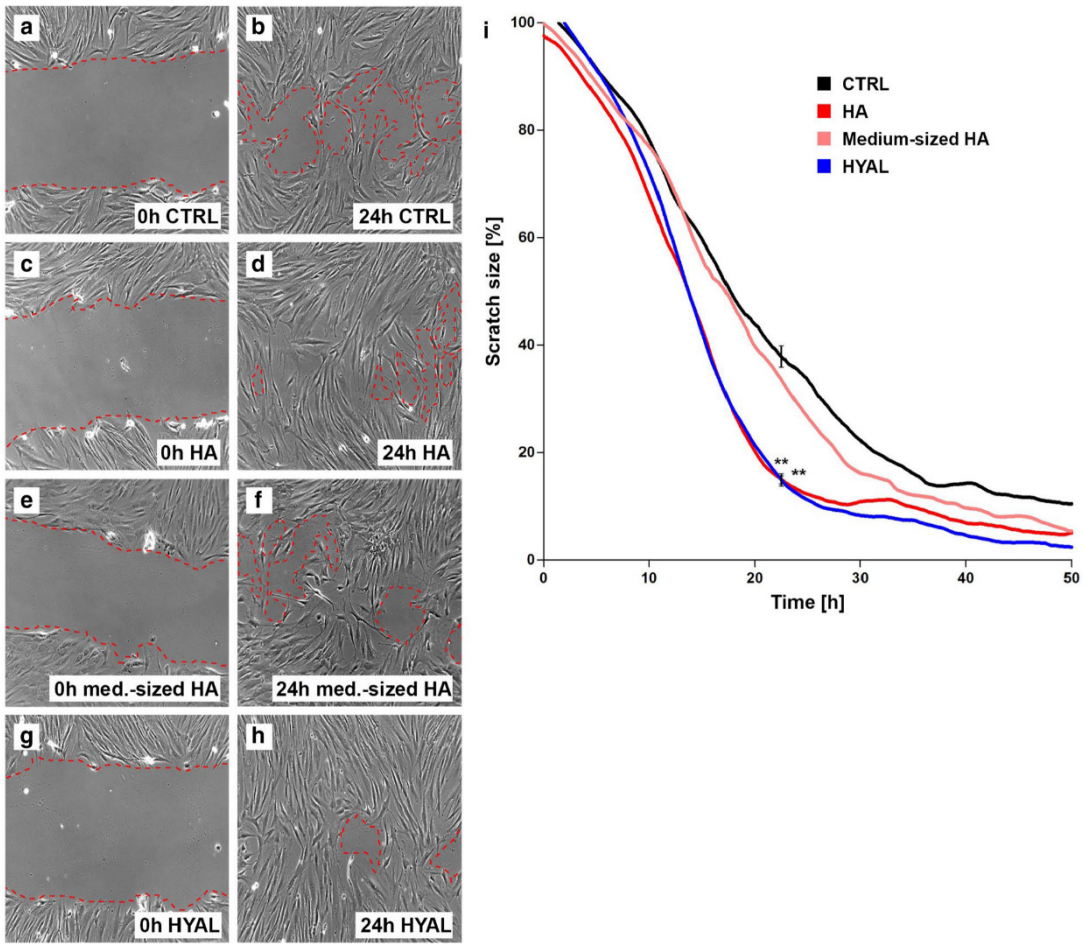

Fig. 3 HA and HYAL accelerate wound closure in an in vitro model. Standardized in vitro wound healing model induced by scratching ("wound scratch assay") a NHDF monolayer of medium control (**a** 0 h, **b** 24 h; black line in **i**), in the presence of HA (1 mg/ml) (**c** 0 h, **d** 24 h; red line in **i**), or medium-sized HA (**e** 0 h, **f** 24 h; pink line in **i**), and HYAL (1.5 U/ml) (**g** 0 h, **h** 24 h; blue line in **i**). The documentation of the wound closure took place over 50 h by means of time-lapse video microscopy. **a**–**h** Show representative images of computer-assisted quantification of the wound area (dotted red line). Values in **i** show percent of scratch size compared to initial scratch size representing the mean of three independent experiments, $*p \leq 0.05$, $**p \leq 0.01$, $***p \leq 0.001$ (*t*-test, two-sided) ($n = 3$)

HA was the highest in cells treated with in low doses of HYAL. Furthermore, immunohistochemical analyses of human skin samples incubated with HYAL ex vivo demonstrated that low concentrations of HYAL (0.015 U/ml) led to a pronounced accumulation of HA, whereas high concentrations of HYAL (15 U/ml) reduced dermal HA levels. In similar observations Philipson et al. [43] found that HYAL treatment at very low concentrations stimulated HA synthesis not only in cultured cells but also in isolated membrane preparations [42] suggesting an existing feedback mechanism that enables cells to sense levels of HA that has been synthesized [49]. The exogenously added HYAL cleaves newly synthesized HA chains as they are being extruded through pore-like structures out of the cell into the extracellular space [44] leaving a message for fibroblasts that insufficient quantities of HA have been synthesized which might result in induced HA synthesis [50]. As early as 1986 Mian postulated the existence of a multi-protein-membrane associated complex that is able to synthesize HA but also has catabolic activity [35, 36]. Two decades later Stern suggested a name for this mini-organelle—the hyaluronasome [49].

Comparable to glycogen granules formed in muscle and liver, the hyaluronasome might respond dynamically to extracellular and intracellular events being able to regulate levels of HA deposition [49]. An organelle in which all components are tethered together (containing HA receptors such as RHAMM and CD44 and HAS but also HYAL and HA-binding proteins) would provide the structural organization for such reactions to occur with maximum efficiency [49, 56]. The existence of a multiplayer like the hyaluronasome could be a reason why HYAL in its lowest concentration is rather able to modulate and stimulate HA-metabolism in a positive feedback loop (see also Fig. 4), compared to high dose HYAL which would rather lead to a total breakdown of all available HA as demonstrated in our ELISA experiments (Fig. 2).

There is a dynamic feedback signaling between HYAL and HAS regulating the net deposition of HA and HA fragments [21, 54, 59]. Out of a variety of cells, dermal fibroblasts are known to synthesize the largest amounts of HA as compared to other cells of the human organism [32]. In line with this observation, in our study NHDF had a higher basal HA production in contrast to epidermal keratinocytes.

The role of HA and HYAL during wound repair is only poorly described. The healing of cutaneous wounds is a complex biological process that can be divided into different phases that overlap in time and space: hemostasis, inflammation, proliferation, and tissue remodeling [18]. Depending on the basis of its molecular weight, HA can produce different effects [13]. At earlier phases of wound healing in vivo, particular high-molecular weight HA increases at the wounding bed to bind fibrinogen which is essential for clot formation [9, 12]. Later on, in the inflammatory stage of wound healing especially low-molecular weight HA accumulates at the wounding site which is in parts generated from high-molecular weight degradation by increasing levels of wound-produced HYAL [12, 15, 41]. These HA fragments then orchestrate specific size-dependent functions [53]. Extensive literature describes that application of exogenous HA can improve wound healing [1, 3, 7, 28]. In the wound healing analyzes presented here, application of HA induced a significant increase in wound closure. Interestingly, scratch closure occurred as fast in the presence of HYAL. In line with these results, Fronza et al. [18] found that not only HA but also HYAL can accelerate wound closure. In contrast to our in vitro based assay using human primary cells their group used an in vivo full-thickness excisional model in Wistar rats. As a HA degrading enzyme HYAL may contribute to the balance between synthesis and deposition of HA and may therefore play a potential role as a healing promoting agent for cutaneous injuries [18]. Decreased wound healing with age is attributed in part to compromised HA metabolism and decreased ability to process HA [34, 52]. In the aged rat skin, studies have found abundance of HMW-HA, perhaps reflecting an inability to generate lower-molecular-size fragments [46]. The lack to generate such small fragments would compromise the wound healing process [3]. Voorhees and Fisher found that the injection of HA-fillers stimulates localized proliferation of fibroblasts in the human skin [45, 57]. These fibroblasts showed a stretched appearance, and expressed high levels of type I procollagen thereby restoring dermal matrix components that are lost in photodamaged skin [16]. When HYAL is added to the wound scratches it might break cross-links in HA which is being extruded in the medium so it behaves like native HA. Possibly, increased concentration of HA fragments resulting from HYAL activity might be important in the wounding process as they stimulate capacity of fibroblast for functional activation. Particularly low-molecular weight HA has been suggested to contribute to wound healing [59]. Therefore, we also investigated the effects of medium-sized HA on wound closure. Surprisingly, medium-sized fragments did not shorten the closure time of the scratch compared to medium control. As other fragment sizes were not investigated in our study, this could be addressed in future studies.

Wohlrab et al. investigated the influence of adjuvant HYAL on wound healing in a placebo-controlled, double-blinded clinical trial. Regarding target parameters like transepidermal water loss, hemovascular perfusion, and complete macroscopic epithelization of the wound his group found no evidence that HYAL retards wound healing [60].

To conclude, HYAL is a bioactive enzyme that exerts multiple effects on the HA-metabolism as well as on the structural cells of the skin. Our study provides direct evidence that especially low doses of HYAL significantly induce HAS and as well as the synthesis and concentration of HA whereas high-dose-HYAL leads to a downmodulation of HA in dermal fibroblasts. Thus, low-dose-HYAL may be beneficial in the rejuvenation of aged skin as it stimulates dermal fibroblasts to increase HA amount. In addition, our study points toward an important role of HYAL in wound healing as HYAL accelerates wound closure in an in vitro wound scratch model of dermal fibroblasts. Future studies are required to further fully elucidate the underlying molecular pathways of HYAL and HA action in the skin.

Supplementary information

Supplementary information accompanies this paper at https://doi.org/10.1186/s40001-020-00460-z.

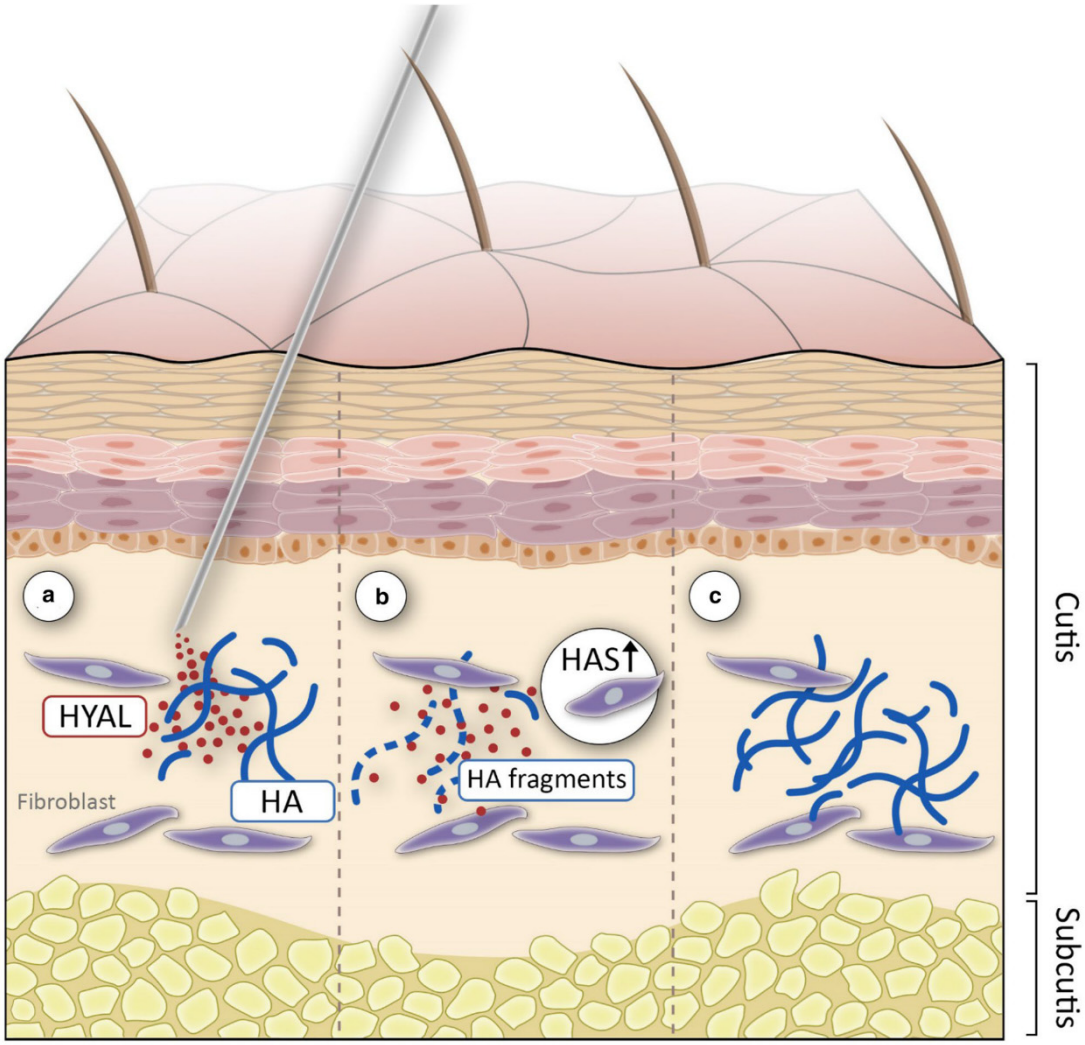

Fig. 4 Injection of low-dose HYAL (**a**) degrades HA in the extracellular matrix of the skin (**b**). HYAL and breakdown fragments of HA might be involved in induction of HA synthases resulting in accumulation of HA in the skin (**c**)

Additional file 1: Table S1. Affymetrix® expression analysis of NHDF treated with HA vs. control showing the 50 most upregulated genes (FC = fold change). **Table S2.** Affymetrix® expression analysis of NHDF treated with HA vs. control showing the 50 most downregulated genes (FC = fold change). **Table S3.** Affymetrix® expression analysis of NHDF treated with medium-sized HA vs. control showing the 50 most upregulated genes (FC = fold change). **Table S4.** Affymetrix® expression analysis of NHDF treated with medium-sized HA vs. control showing the 50 most downregulated genes (FC = fold change). **Table S5.** Affymetrix® expression analysis of NHDF treated with HYAL vs. control showing the 50 most upregulated genes (FC = fold change). **Table S6.** Affymetrix® expression analysis of NHDF treated with HYAL vs. control showing the 50 most downregulated genes (FC = fold change). **Figure S1.** (A, C) HAS1, HAS3 gene expression levels in normal human dermal fibroblasts (NHDF) after stimulation with 1 mg/ml HA, 1.5 U/ml HYAL and HA + HYAL co-stimulation for 2 h, 4 h, 12 h and 24 h, (B, D) HAS1, HAS3 gene expression levels of NHDF after stimulation with 15 U/ml, 1.5 U/ml, 0.15 U/ml and 0.015 U/ml HYAL for 24 h. Asterisks above columns indicate statistical significant differences compared to their respective medium controls. $*p \leq 0.05$, $**p \leq 0.01$, $***p \leq 0.001$ (*t*-test, two-sided). **Figure S2.** (A, C, E) HAS1, HAS2, HAS3 gene expression levels in primary human keratinocytes after stimulation with 1 mg/ml HA, 1.5 U/ml HYAL and HA + HYAL co-stimulation for 2 h, 4 h, 12 h and 24 h, (B, D, F) HAS1, HAS2, HAS3 gene expression levels in keratinocytes after stimulation with 15 U/ml, 1.5 U/ml, 0.15 U/ml and 0.015 U/ml HYAL for 24 h, (G, H) HA amount (ng/ml) measurement by means of ELISA in supernatants of NHDF treated as described in A–F. Asterisks above columns indicate statistical significant differences

compared to their respective medium controls. *$p \leq 0.05$, **$p \leq 0.01$, ***$p \leq 0.001$ (*t*-test, two-sided).

Authors' contributions
BAB designed and performed the experiments and wrote the paper. HS, KG, OR and JWF provided expertise especiallyon hyaluronan ELISA and immunohistochemistry. BH, PAG and EB designed the experiments, gave conceptual advice,and contributed significantly to the data analyses, interpretion of the results, and edited the paper. All authors read andapproved the final manuscript.

Funding
Open Access funding enabled and organized by Projekt DEAL. The project was supported by a research grant by Riemser Pharma, Greifswald, Germany.

Availability of data and materials
All data and materials can be accessed via BB and PAG.

Ethics approval and consent to participate
The work was approved by the local ethical review board.

Consent for publication
All authors gave consent for the publication.

Competing interests
BAB and PAG have received research funding by Riemser Pharma. PAG has received honoraria for presentations by Riemser Pharma.

Author details
[1] Department of Dermatology, University Hospital Duesseldorf, Duesseldorf, Germany. [2] Department of Pharmacology, University Hospital Duesseldorf, Duesseldorf, Germany. [3] Department of Radiation Oncology, Medical Faculty, University Hospital Duesseldorf, Duesseldorf, Germany. [4] Dermatologie am Luegplatz, Duesseldorf, Germany.

Received: 30 August 2020 Accepted: 12 November 2020
Published online: 23 November 2020

References

1. Averbeck M, Gebhardt C, Anderegg U, Simon JC. Suppression of hyaluronan synthase 2 expression reflects the anthropogenic potential of glucocorticoids. Exp Dermatol. 2010;19:757–9.
2. Averbeck M, Gebhardt CA, Voigt S, Beilharz S, Anderegg U, Termeer CC, Sleeman JP, Simon JC. Differential regulation of hyaluronan metabolism in the epidermal and dermal compartments of human skin by UVB irradiation. J Invest Dermatol. 2007;127:687–97.
3. Aya KL, Stern R. Hyaluronan in wound healing: rediscovering a major player. Wound Repair Regen. 2014;22:579–93.
4. Barrientos S, Stojadinovic O, Golinko MS, Brem H, Tomic-Canic M. Growth factors and cytokines in wound healing. Wound Repair Regen. 2008;16:585–601.
5. Bissell MJ, Hall HG, Parry G. How does the extracellular matrix direct gene expression? J Theor Biol. 1982;99:31–68.
6. Buhren BA, Schrumpf H, Hoff NP, Bolke E, Hilton S, Gerber PA. Hyaluronidase: from clinical applications to molecular and cellular mechanisms. Eur J Med Res. 2016;21:5.
7. Byl NN, Mckenzie A, West J, Stern M, Halliday B, Stern R, Wong T. Amniotic fluid enhances wound healing—a randomized controlled three week trial in mini Yucatan pigs. Eur J Phys Med Rehab. 1993;3:105–13.
8. Camenisch TD, Schroeder JA, Bradley J, Klewer SE, Mcdonald JA. Heart-valve mesenchyme formation is dependent on hyaluronan-augmented activation of ErbB2-ErbB3 receptors. Nat Med. 2002;8:850–5.
9. Chen WY, Abatangelo G. Functions of hyaluronan in wound repair. Wound Repair Regen. 1999;7:79–89.
10. Ciccone V, Zazzetta M, Morbidelli L. Comparison of the effect of two hyaluronic acid preparations on fibroblast and endothelial cell functions related to angiogenesis. Cells. 2019;8:1479.
11. Csoka AB, Frost GI, Stern R. The six hyaluronidase-like genes in the human and mouse genomes. Matrix Biol. 2001;20:499–508.
12. D'agostino A, Stellavato A, Busico T, Papa A, Tirino V, Papaccio G, La Gatta A, De Rosa M, Schiraldi C. In vitro analysis of the effects on wound healing of high- and low-molecular weight chains of hyaluronan and their hybrid H-HA/L-HA complexes. BMC Cell Biol. 2015;16:19.
13. David-Raoudi M, Tranchepain F, Deschrevel B, Vincent JC, Bogdanowicz P, Boumediene K, Pujol JP. Differential effects of hyaluronan and its fragments on fibroblasts: relation to wound healing. Wound Repair Regen. 2008;16:274–87.
14. Delmage JM, Powars DR, Jaynes PK, Allerton SE. The selective suppression of immunogenicity by hyaluronic acid. Ann Clin Lab Sci. 1986;16:303–10.
15. Dunphy JE, Udupa KN. Chemical and histochemical sequences in the normal healing of wounds. N Engl J Med. 1955;253:847–51.
16. Fisher GJ, Varani J, Voorhees JJ. Looking older: fibroblast collapse and therapeutic implications. Arch Dermatol. 2008;144:666–72.
17. Flynn TC, Thompson DH, Hyun SH. Molecular weight analyses and enzymatic degradation profiles of the soft-tissue fillers Belotero Balance, Restylane, and Juvederm Ultra. Plast Reconstr Surg. 2013;132:22s–32s.
18. Fronza M, Caetano GF, Leite MN, Bitencourt CS, Paula-Silva FW, Andrade TA, Frade MA, Merfort I, Faccioli LH. Hyaluronidase modulates inflammatory response and accelerates the cutaneous wound healing. PLoS ONE. 2014;9:E112297.
19. Funt D, Pavicic T. Dermal fillers in aesthetics: an overview of adverse events and treatment approaches. Clin Cosmet Investig Dermatol. 2013;6:295–316.
20. Heldin P, Laurent TC, Heldin CH. Effect of growth factors on hyaluronan synthesis in cultured human fibroblasts. Biochem J. 1989;258:919–22.
21. Heldin P, Basu K, Olofsson B, Porsch H, Kozlova I, Kahata K. Deregulation of hyaluronan synthesis, degradation and binding promotes breast cancer. J Biochem. 2013;154:395–408.
22. Hirsch RJ, Brody HJ, Carruthers JD. Hyaluronidase in the office: a necessity for every dermasurgeon that injects hyaluronic acid. J Cosmet Laser Ther. 2007;9:182–5.
23. Homey B, Dieu-Nosjean MC, Wiesenborn A, Massacrier C, Pin JJ, Oldham E, Catron D, Buchanan ME, Muller A, Dewaal Malefyt R, Deng G, Orozco R, Ruzicka T, Lehmann P, Lebecque S, Caux C, Zlotnik A. Up-regulation of macrophage inflammatory protein-3 alpha/CCL20 and CC chemokine receptor 6 in psoriasis. J Immunol. 2000;164:6621–32.
24. Isnard N, Legeais JM, Renard G, Robert L. Effect of hyaluronan on MMP expression and activation. Cell Biol Int. 2001;25:735–9.
25. Jahn K, Homey B, Gerber PA. Management of complications after aesthetic hyaluronic acid injections. Hautarzt. 2014;65:851–3.
26. Juhlin L. Hyaluronan in skin. J Intern Med. 1997;242:61–6.
27. Kaya G, Tran C, Sorg O, Hotz R, Grand D, Carraux P, Didierjean L, Stamenkovic I, Saurat JH. Hyaluronate fragments reverse skin atrophy by a CD44-dependent mechanism. Plos Med. 2006;3:E493.
28. King SR, Hickerson WL, Proctor KG. Beneficial actions of exogenous hyaluronic acid on wound healing. Surgery. 1991;109:76–84.
29. Larnier C, Kerneur C, Robert L, Moczar M. Effect of testicular hyaluronidase on hyaluronate synthesis by human skin fibroblasts in culture. Biochim Biophys Acta. 1989;1014:145–52.
30. Laurent TC, Fraser JR. The properties and turnover of hyaluronan. Ciba Found Symp. 1986;124:9–29.
31. Laurent TC, Fraser JR. Hyaluronan. FASEB J. 1992;6:2397–404.
32. Li L, Asteriou T, Bernert B, Heldin CH, Heldin P. Growth factor regulation of hyaluronan synthesis and degradation in human dermal fibroblasts: importance of hyaluronan for the mitogenic response of PDGF-BB. Biochem J. 2007;404:327–36.
33. Lichtenberger BM, Gerber PA, Holcmann M, Buhren BA, Amberg N, Smolle V, Schrumpf H, Boelke E, Ansari P, Mackenzie C, Wollenberg A, Kislat A, Fischer JW, Rock K, Harder J, Schroder JM, Homey B, Sibilia M. Epidermal EGFR controls cutaneous host defense and prevents inflammation. Sci Transl Med. 2013;5:199111.
34. Meyer LJ, Stern R. Age-dependent changes of hyaluronan in human skin. J Invest Dermatol. 1994;102:385–9.
35. Mian N. Analysis of cell-growth-phase-related variations in hyaluronate synthase activity of isolated plasma-membrane fractions of cultured human skin fibroblasts. Biochem J. 1986a;237:333–42.

36. Mian N. Characterization of a high-Mr plasma-membrane-bound protein and assessment of its role as a constituent of hyaluronate synthase complex. Biochem J. 1986b;237:343–57.
37. Moczar M, Robert L. Stimulation of cell proliferation by hyaluronidase during in vitro aging of human skin fibroblasts. Exp Gerontol. 1993;28:59–68.
38. Monsuur HN, Boink MA, Weijers EM, Roffel S, Breetveld M, Gefen A, Van Den Broek LJ, Gibbs S. Methods to study differences in cell mobility during skin wound healing in vitro. J Biomech. 2016;49:1381–7.
39. Nair AB, Jacob S. A simple practice guide for dose conversion between animals and human. J Basic Clin Pharm. 2016;7:27–31.
40. Narayanan R, Kuppermann BD. Hyaluronidase for pharmacologic vitreolysis. Dev Ophthalmol. 2009;44:20–5.
41. Noble PW. Hyaluronan and its catabolic products in tissue injury and repair. Matrix Biol. 2002;21:25–9.
42. Philipson LH, Schwartz NB. Subcellular localization of hyaluronate synthetase in oligodendroglioma cells. J Biol Chem. 1984;259:5017–23.
43. Philipson LH, Westley J, Schwartz NB. Effect of hyaluronidase treatment of intact cells on hyaluronate synthetase activity. Biochemistry. 1985;24:7899–906.
44. Prehm P. Release of hyaluronate from eukaryotic cells. Biochem J. 1990;267:185–9.
45. Quan T, Wang F, Shao Y, Rittie L, Xia W, Orringer JS, Voorhees JJ, Fisher GJ. Enhancing structural support of the dermal microenvironment activates fibroblasts, endothelial cells, and keratinocytes in aged human skin in vivo. J Invest Dermatol. 2013;133:658–67.
46. Reed MJ, Damodarasamy M, Chan CK, Johnson MN, Wight TN, Vernon RB. Cleavage of hyaluronan is impaired in aged dermal wounds. Matrix Biol. 2013;32:45–51.
47. Rock K, Grandoch M, Majora M, Krutmann J, Fischer JW. Collagen fragments inhibit hyaluronan synthesis in skin fibroblasts in response to ultraviolet B (UVB): new insights into mechanisms of matrix remodeling. J Biol Chem. 2011;286:18268–76.
48. Sharma V, Mcneill JH. To scale or not to scale: the principles of dose extrapolation. Br J Pharmacol. 2009;157:907–21.
49. Stern R. Devising a pathway for hyaluronan catabolism: are we there yet? Glycobiology. 2003;13:105r–15r.
50. Stern R. Hyaluronan catabolism: a new metabolic pathway. Eur J Cell Biol. 2004;83:317–25.
51. Stern R, Jedrzejas MJ. Hyaluronidases: their genomics, structures, and mechanisms of action. Chem Rev. 2006;106:818–39.
52. Stern R, Maibach HI. Hyaluronan in skin: aspects of aging and its pharmacologic modulation. Clin Dermatol. 2008;26:106–22.
53. Stern R, Asari AA, Sugahara KN. Hyaluronan fragments: an information-rich system. Eur J Cell Biol. 2006;85:699–715.
54. Takahashi Y, Li L, Kamiryo M, Asteriou T, Moustakas A, Yamashita H, Heldin P. Hyaluronan fragments induce endothelial cell differentiation in a CD44- and CXCL1/GRO1-dependent manner. J Biol Chem. 2005;280:24195–204.
55. Tian X, Azpurua J, Hine C, Vaidya A, Myakishev-Rempel M, Ablaeva J, Mao Z, Nevo E, Gorbunova V, Seluanov A. High-molecular-mass hyaluronan mediates the cancer resistance of the naked mole rat. Nature. 2013;499:346–9.
56. Wahby A, Dicaprio KD, Stern R. Hyaluronan inside and outside of skin. In: Lodén M, Maibach H, editors. Treatment of dry skin syndrome. Berlin: Springer; 2012.
57. Wang F, Garza LA, Kang S, Varani J, Orringer JS, Fisher GJ, Voorhees JJ. In vivo stimulation of de novo collagen production caused by cross-linked hyaluronic acid dermal filler injections in photodamaged human skin. Arch Dermatol. 2007;143:155–63.
58. Weber GC, Buhren BA, Schrumpf H, Wohlrab J, Gerber PA. Clinical applications of hyaluronidase. Adv Exp Med Biol. 2019;1148:255–77.
59. West DC, Hampson IN, Arnold F, Kumar S. Angiogenesis induced by degradation products of hyaluronic acid. Science. 1985;228:1324–6.
60. Wohlrab J, Finke R, Franke WG, Wohlrab A. Clinical trial for safety evaluation of hyaluronidase as diffusion enhancing adjuvant for infiltration analgesia of skin with lidocaine. Dermatol Surg. 2012;38:91–6.

Publisher's Note

Table S1. Affymetrix® expression analysis of NHDF treated with HA vs. control showing the 50 most upregulated genes (FC = fold change).

Rank	FC (abs) HA vs. Control (UP)	Gene Symbol	Gene Title
1	1,9477	CLDN4	claudin 4
2	1,9008	LCE2A	late cornified envelope 2A
3	1,8966	RTN1	reticulon 1
4	1,8899	MT1G	metallothionein 1G
5	1,8481	SMARCD1	SWI/SNF related, matrix associated, actin dependent regulator of chromatin, subfamily d, member 1
6	1,8355	NEDD4L	neural precursor cell expressed, developmentally down-regulated 4-like, E3 ubiquitin protein ligase
7	1,8326	FGD2	FYVE, RhoGEF and PH domain containing 2
8	1,8222	NUDCD3	NudC domain containing 3
9	1,8137	B3GNT7	UDP-GlcNAc:betaGal beta-1,3-N-acetylglucosaminyltransferase 7
10	1,7957	AGBL4	ATP/GTP binding protein-like 4
11	1,7682	LCE3A	late cornified envelope 3A
12	1,7667	DUOXA1	dual oxidase maturation factor 1
13	1,7642	FXYD5	FXYD domain containing ion transport regulator 5
14	1,7523	FAM131B	family with sequence similarity 131, member B
15	1,7481	HBEGF	heparin-binding EGF-like growth factor
16	1,7476	DNAI2	dynein, axonemal, intermediate chain 2
17	1,7392	INSC	inscuteable homolog (Drosophila)
18	1,7361	ALPK3	alpha-kinase 3
19	1,7336	LCE3D	late cornified envelope 3D
20	1,7283	RIMS1	regulating synaptic membrane exocytosis 1
21	1,7111	YIF1B	Yip1 interacting factor homolog B (S. cerevisiae)
22	1,7082	GUCA1A	guanylate cyclase activator 1A (retina)
23	1,7056	TNNT3	troponin T type 3 (skeletal, fast)
24	1,7033	CRIP3	cysteine-rich protein 3
25	1,7022	VRK3	vaccinia related kinase 3
26	1,6998	BEST1	bestrophin 1
27	1,6993	CORO1A	coronin, actin binding protein, 1A
28	1,6886	LOC100505815	uncharacterized LOC100505815
29	1,6882	CDH22	cadherin 22, type 2
30	1,6844	SNORA5B	small nucleolar RNA, H/ACA box 5B (transforming growth factor beta regulator 4)
31	1,6828	C10orf25	chromosome 10 open reading frame 25
32	1,6790	MAP3K9	mitogen-activated protein kinase kinase kinase 9
33	1,6773	COX19	COX19 cytochrome c oxidase assembly homolog (S. cerevisiae)
34	1,6771	YME1L1	YME1-like 1 (S. cerevisiae)
35	1,6766	C14orf182	chromosome 14 open reading frame 182
36	1,6689	LRRC37A11P	leucine rich repeat containing 37, member A11, pseudogene
37	1,6677	ATPAF2	ATP synthase mitochondrial F1 complex assembly factor 2
38	1,6647	TDRKH	tudor and KH domain containing
39	1,6534	CRISP1	cysteine-rich secretory protein 1
40	1,6456	C8orf46	chromosome 8 open reading frame 46
41	1,6448	PRKG2	protein kinase, cGMP-dependent, type II
42	1,6404	C1orf229	chromosome 1 open reading frame 229
43	1,6392	ALS2CL	ALS2 C-terminal like
44	1,6367	ZNF496	Zinc finger protein 496
45	1,6350	MRGPRX2	MAS-related GPR, member X2
46	1,6341	OR2T3	olfactory receptor, family 2, subfamily T, member 3
47	1,6324	ERVK3-2	endogenous retrovirus group K3, member 2
48	1,6282	MAPK15	mitogen-activated protein kinase 15
49	1,6265	SGK2	serum/glucocorticoid regulated kinase 2
50	1,6239	THUMPD3	THUMP domain containing 3

Table S2. Affymetrix® expression analysis of NHDF treated with HA vs. control showing the 50 most downregulated genes (FC = fold change).

Rank	FC (abs) HA vs. Control (DOWN)	Gene Symbol	Gene Title
1	3,8311	CXCL5	chemokine (C-X-C motif) ligand 5
2	2,7615	DYNC1I2	dynein, cytoplasmic 1, intermediate chain 2
3	2,3244	COX1	cytochrome c oxidase subunit I
4	2,3046	HNRNPM	heterogeneous nuclear ribonucleoprotein M
5	2,1574	IL7	interleukin 7
6	2,1018	SPRY4	sprouty homolog 4 (Drosophila)
7	2,0670	SNORA12	small nucleolar RNA, H/ACA box 12
8	2,0338	ND4	NADH dehydrogenase, subunit 4 (complex I)
9	2,0312	ETV1	ets variant 1
10	2,0266	C10orf54	chromosome 10 open reading frame 54
11	2,0166	MYH9	myosin, heavy chain 9, non-muscle
12	2,0077	SIPA1L2	signal-induced proliferation-associated 1 like 2
13	1,9980	FNDC3B	fibronectin type III domain containing 3B
14	1,9944	MTR	5-methyltetrahydrofolate-homocysteine methyltransferase
15	1,9879	HMGN5	high mobility group nucleosome binding domain 5
16	1,9662	MCM8	minichromosome maintenance complex component 8
17	1,9374	ANKRD36	ankyrin repeat domain 36
18	1,9331	COX3	cytochrome c oxidase III
19	1,9192	SLC40A1	solute carrier family 40 (iron-regulated transporter), member 1
20	1,8910	TRUB1	TruB pseudouridine (psi) synthase homolog 1 (E. coli)
21	1,8827	ZNF345	zinc finger protein 345
22	1,8824	PIM1	pim-1 oncogene
23	1,8702	NPIP	nuclear pore complex interacting protein
24	1,8348	COL14A1	collagen, type XIV, alpha 1
25	1,8319	ZNF563	zinc finger protein 563
26	1,8276	LOC157503	uncharacterized LOC157503
27	1,8248	KCNQ1OT1	KCNQ1 opposite strand/antisense transcript 1 (non-protein coding)
28	1,8158	STK4	serine/threonine kinase 4
29	1,8079	SLC38A4	solute carrier family 38, member 4
30	1,8043	CHD2	chromodomain helicase DNA binding protein 2
31	1,8036	MAFB	v-maf musculoaponeurotic fibrosarcoma oncogene homolog B (avian)
32	1,7967	MALAT1	metastasis associated lung adenocarcinoma transcript 1 (non-protein coding)
33	1,7956	DKK2	dickkopf 2 homolog (Xenopus laevis)
34	1,7910	VCAN	versican
35	1,7880	CLK4	CDC-like kinase 4
36	1,7854	TMPO	thymopoietin
37	1,7787	USP15	ubiquitin specific peptidase 15
38	1,7731	MTMR12	myotubularin related protein 12
39	1,7691	AFF4	AF4/FMR2 family, member 4
40	1,7677	ZC3H7A	zinc finger CCCH-type containing 7A
41	1,7657	SKP2	S-phase kinase-associated protein 2, E3 ubiquitin protein ligase
42	1,7550	SVIP	small VCP/p97-interacting protein
43	1,7517	CACUL1	CDK2-associated, cullin domain 1
44	1,7514	SLAMF6	SLAM family member 6
45	1,7506	PKD1P1	polycystic kidney disease 1 (autosomal dominant) pseudogene 1
46	1,7463	SMG1	smg-1 homolog, phosphatidylinositol 3-kinase-related kinase (C. elegans)
47	1,7431	CDK1	cyclin-dependent kinase 1
48	1,7417	CDKN3	cyclin-dependent kinase inhibitor 3
49	1,7381	DNAJC9	DnaJ (Hsp40) homolog, subfamily C, member 9
50	1,7362	ANKRD44	ankyrin repeat domain 44

Table S3. Affymetrix® expression analysis of NHDF treated with medium-sized HA vs. control showing the 50 most upregulated genes (FC = fold change).

Rank	FC (abs) HA medium size vs. Control (UP)	Gene Symbol	Gene Title
1	2,2189	CCDC64B	coiled-coil domain containing 64B
2	2,1718	FAM96A	family with sequence similarity 96, member A
3	2,0896	TAC4	tachykinin 4 (hemokinin)
4	1,9934	RPL5	ribosomal protein L5
5	1,9530	INSC	inscuteable homolog (Drosophila)
6	1,8931	SPATA6	spermatogenesis associated 6
7	1,8682	FEZ1	fasciculation and elongation protein zeta 1 (zygin I)
8	1,8657	C10orf128	chromosome 10 open reading frame 128
9	1,8623	ADRBK2	adrenergic, beta, receptor kinase 2
10	1,8515	KRT71	keratin 71
11	1,8443	UBXN1	UBX domain protein 1
12	1,8385	RPL34-AS1	RPL34 antisense RNA 1 (non-protein coding)
13	1,8363	GGT1	gamma-glutamyltransferase 1
14	1,8154	NEDD4L	neural precursor cell expressed, developmentally down-regulated 4-like, E3 ubiquitin protein ligase
15	1,8134	OR2H1	olfactory receptor, family 2, subfamily H, member 1
16	1,7982	CPNE6	copine VI (neuronal)
17	1,7963	FAM189A1	family with sequence similarity 189, member A1
18	1,7884	ADORA2A	adenosine A2a receptor
19	1,7882	SPATA6L	spermatogenesis associated 6-like
20	1,7852	VWDE	von Willebrand factor D and EGF domains
21	1,7831	DNMT3L	DNA (cytosine-5-)-methyltransferase 3-like
22	1,7775	ATPAF2	ATP synthase mitochondrial F1 complex assembly factor 2
23	1,7565	HNMT	histamine N-methyltransferase
24	1,7525	C10orf53	chromosome 10 open reading frame 53
25	1,7489	CAPN6	calpain 6
26	1,7450	NDUFS2	NADH dehydrogenase (ubiquinone) Fe-S protein 2, 49kDa (NADH-coenzyme Q reductase)
27	1,7435	SLC25A2	solute carrier family 25 (mitochondrial carrier; ornithine transporter) member 2
28	1,7430	C7orf10	chromosome 7 open reading frame 10
29	1,7430	PIK3AP1	phosphoinositide-3-kinase adaptor protein 1
30	1,7412	SLC16A14	solute carrier family 16, member 14 (monocarboxylic acid transporter 14)
31	1,7306	SNORA14B	small nucleolar RNA, H/ACA box 14B
32	1,7230	DMKN	dermokine
33	1,7176	DNAJB2	DnaJ (Hsp40) homolog, subfamily B, member 2
34	1,7169	BCL2L15	BCL2-like 15
35	1,7165	TNNT3	troponin T type 3 (skeletal, fast)
36	1,7154	FLJ39061	uncharacterized protein FLJ39061
37	1,7087	PDZD7	PDZ domain containing 7
38	1,7063	TAC3	tachykinin 3
39	1,7029	HEXA	hexosaminidase A (alpha polypeptide)
40	1,7009	FRY	furry homolog (Drosophila)
41	1,7007	MCTP2	multiple C2 domains, transmembrane 2
42	1,6898	GLP2R	glucagon-like peptide 2 receptor
43	1,6882	GHRL	ghrelin/obestatin prepropeptide
44	1,6810	GLS2	glutaminase 2 (liver, mitochondrial)
45	1,6784	PEX26	peroxisomal biogenesis factor 26
46	1,6761	LRRC37A11P	leucine rich repeat containing 37, member A11, pseudogene
47	1,6727	SLC25A41	solute carrier family 25, member 41
48	1,6702	VGLL1	vestigial like 1 (Drosophila)
49	1,6694	NAIF1	nuclear apoptosis inducing factor 1
50	1,6642	SEC14L4	SEC14-like 4 (S. cerevisiae)

Table S4. Affymetrix® expression analysis of NHDF treated with medium-sized HA vs. control showing the 50 most downregulated genes (FC = fold change).

Rank	FC (abs) HA medium size vs. Control (DOWN)	Gene Symbol	Gene Title
1	2,6306	USP15	ubiquitin specific peptidase 15
2	2,3820	CDKN3	cyclin-dependent kinase inhibitor 3
3	2,1296	TAX1BP1	Tax1 (human T-cell leukemia virus type I) binding protein 1
4	2,1153	PNISR	PNN-interacting serine/arginine-rich protein
5	2,0955	SNORA12	small nucleolar RNA, H/ACA box 12
6	2,0452	NUMB	numb homolog (Drosophila)
7	1,9578	MYSM1	Myb-like, SWIRM and MPN domains 1
8	1,9439	CPM	carboxypeptidase M
9	1,8921	TMEM50B	transmembrane protein 50B
10	1,8815	ANKRD36	ankyrin repeat domain 36
11	1,8757	TMEM65	transmembrane protein 65
12	1,8682	TRMT13	tRNA methyltransferase 13 homolog (S. cerevisiae)
13	1,8670	SNAPC1	small nuclear RNA activating complex, polypeptide 1, 43kDa
14	1,8355	CHORDC1	cysteine and histidine-rich domain (CHORD) containing 1
15	1,8305	CCPG1	cell cycle progression 1
16	1,8202	C7orf41	chromosome 7 open reading frame 41
17	1,8115	CHIC1	cysteine-rich hydrophobic domain 1
18	1,7970	COL5A2	collagen, type V, alpha 2
19	1,7965	NEK2	NIMA (never in mitosis gene a)-related kinase 2
20	1,7961	SUCLG2	succinate-CoA ligase, GDP-forming, beta subunit
21	1,7877	FAM46C	family with sequence similarity 46, member C
22	1,7869	ITGAV	integrin, alpha V
23	1,7845	MAFB	v-maf musculoaponeurotic fibrosarcoma oncogene homolog B (avian)
24	1,7806	DST	dystonin
25	1,7722	ILF3	interleukin enhancer binding factor 3, 90kDa
26	1,7666	VCAN	versican
27	1,7581	ZBED4	zinc finger, BED-type containing 4
28	1,7570	SORBS2	sorbin and SH3 domain containing 2
29	1,7561	MTHFD2L	methylenetetrahydrofolate dehydrogenase (NADP+ dependent) 2-like
30	1,7560	LOC100131541	uncharacterized LOC100131541
31	1,7541	GMCL1	germ cell-less homolog 1 (Drosophila)
32	1,7529	CASC4	cancer susceptibility candidate 4
33	1,7516	C15orf29	chromosome 15 open reading frame 29
34	1,7511	MAP9	microtubule-associated protein 9
35	1,7500	TSPAN12	tetraspanin 12
36	1,7378	CEP57	centrosomal protein 57kDa
37	1,7364	DBF4	DBF4 homolog (S. cerevisiae)
38	1,7295	FAM208B	family with sequence similarity 208, member B
39	1,7287	SWAP70	SWAP switching B-cell complex 70kDa subunit
40	1,7163	EMB	embigin
41	1,7156	MKI67	antigen identified by monoclonal antibody Ki-67
42	1,7154	GCC2	GRIP and coiled-coil domain containing 2
43	1,7154	ZBTB1	zinc finger and BTB domain containing 1
44	1,7142	CDC7	cell division cycle 7 homolog (S. cerevisiae)
45	1,7097	COL14A1	collagen, type XIV, alpha 1
46	1,7081	OGN	osteoglycin
47	1,7072	CISD1	CDGSH iron sulfur domain 1
48	1,7048	ZNF345	zinc finger protein 345
49	1,7026	CREBBP	CREB binding protein
50	1,7025	WNT5A	wingless-type MMTV integration site family, member 5A

Table S5. Affymetrix® expression analysis of NHDF treated with HYAL vs. control showing the 50 most upregulated genes (FC = fold change).

Rank	FC (abs) Hylase vs. Control (UP)	Gene Symbol	Gene Title
1	3,3780	RGS16	regulator of G-protein signaling 16
2	2,6295	LCE2A	late cornified envelope 2A
3	2,5560	LCE2C	late cornified envelope 2C
4	2,5431	SERPINB2	serpin peptidase inhibitor, clade B (ovalbumin), member 2
5	2,5383	BMP2	bone morphogenetic protein 2
6	2,4468	IL33	interleukin 33
7	2,3795	CXCL6	chemokine (C-X-C motif) ligand 6 (granulocyte chemotactic protein 2)
8	2,3106	LCE3D	late cornified envelope 3D
9	2,2799	NEFM	neurofilament, medium polypeptide
10	2,2777	LCE3A	late cornified envelope 3A
11	2,2621	LCE1F	late cornified envelope 1F
12	2,2168	TMEM158	transmembrane protein 158 (gene/pseudogene)
13	2,2119	IL11	interleukin 11
14	2,1872	ABCG1	ATP-binding cassette, sub-family G (WHITE), member 1
15	2,1733	GORASP1	golgi reassembly stacking protein 1, 65kDa
16	2,1695	ADRBK2	adrenergic, beta, receptor kinase 2
17	2,1555	STC1	stanniocalcin 1
18	2,0847	CALB2	calbindin 2
19	2,0790	PTHLH	parathyroid hormone-like hormone
20	2,0167	MMP10	matrix metallopeptidase 10 (stromelysin 2)
21	2,0158	RNF152	ring finger protein 152
22	1,9917	NUDCD3	NudC domain containing 3
23	1,9903	SOBP	sine oculis binding protein homolog (Drosophila)
24	1,9852	INSC	inscuteable homolog (Drosophila)
25	1,9818	EDNRB	endothelin receptor type B
26	1,9769	HBEGF	heparin-binding EGF-like growth factor
27	1,9574	NTRK1	neurotrophic tyrosine kinase, receptor, type 1
28	1,9512	PTPN22	protein tyrosine phosphatase, non-receptor type 22 (lymphoid)
29	1,9398	TGFA	transforming growth factor, alpha
30	1,9336	PAPPA	pregnancy-associated plasma protein A, pappalysin 1
31	1,9335	SPRY4	sprouty homolog 4 (Drosophila)
32	1,9303	B3GALT5	UDP-Gal:betaGlcNAc beta 1,3-galactosyltransferase, polypeptide 5
33	1,9145	GPRC5A	G protein-coupled receptor, family C, group 5, member A
34	1,9119	CCDC93	coiled-coil domain containing 93
35	1,9080	P2RX2	purinergic receptor P2X, ligand-gated ion channel, 2
36	1,8950	MMP16	matrix metallopeptidase 16 (membrane-inserted)
37	1,8853	PHLDA1	pleckstrin homology-like domain, family A, member 1
38	1,8840	HSD17B2	hydroxysteroid (17-beta) dehydrogenase 2
39	1,8826	AKAP8	A kinase (PRKA) anchor protein 8
40	1,8680	INHBA	inhibin, beta A
41	1,8667	EPHB1	EPH receptor B1
42	1,8617	ENDOU	endonuclease, polyU-specific
43	1,8583	ALG9	asparagine-linked glycosylation 9, alpha-1,2-mannosyltransferase homolog (S. cerevisiae)
44	1,8549	C14orf182	chromosome 14 open reading frame 182
45	1,8533	RHD	Rh blood group, D antigen
46	1,8492	NEFL	neurofilament, light polypeptide
47	1,8473	FRMD3	FERM domain containing 3
48	1,8439	FAM167A	family with sequence similarity 167, member A
49	1,8425	C20orf173	chromosome 20 open reading frame 173
50	1,8350	IL8	interleukin 8

Table S6. Affymetrix® expression analysis of NHDF treated with HYAL vs. control showing the 50 most downregulated genes (FC = fold change).

Rank	FC (abs) Hylase vs. Control (DOWN)	Gene Symbol	Gene Title
1	2,7781	FLG	filaggrin
2	2,6449	SYNPO2	synaptopodin 2
3	2,5568	HMGN5	high mobility group nucleosome binding domain 5
4	2,5566	MEST	mesoderm specific transcript homolog (mouse)
5	2,5414	SDPR	serum deprivation response
6	2,4855	NEK2	NIMA (never in mitosis gene a)-related kinase 2
7	2,4656	INMT	indolethylamine N-methyltransferase
8	2,3091	ANKRD6	ankyrin repeat domain 6
9	2,2227	PDE5A	phosphodiesterase 5A, cGMP-specific
10	2,2148	MKX	mohawk homeobox
11	2,2043	DEPTOR	DEP domain containing MTOR-interacting protein
12	2,1713	GPD1L	glycerol-3-phosphate dehydrogenase 1-like
13	2,1462	SNORA12	small nucleolar RNA, H/ACA box 12
14	2,1389	THRB	thyroid hormone receptor, beta
15	2,1386	RDH10	retinol dehydrogenase 10 (all-trans)
16	2,1068	IFIT1	interferon-induced protein with tetratricopeptide repeats 1
17	2,1003	CDKN2B	cyclin-dependent kinase inhibitor 2B (p15, inhibits CDK4)
18	2,0870	CHIC1	cysteine-rich hydrophobic domain 1
19	2,0746	ZNF230	zinc finger protein 230
20	2,0614	TSPAN2	tetraspanin 2
21	2,0582	LGR4	leucine-rich repeat containing G protein-coupled receptor 4
22	2,0523	MAN1C1	mannosidase, alpha, class 1C, member 1
23	2,0459	CDKN3	cyclin-dependent kinase inhibitor 3
24	2,0377	TRIM59	tripartite motif containing 59
25	2,0259	DBF4	DBF4 homolog (S. cerevisiae)
26	2,0224	BCHE	butyrylcholinesterase
27	2,0221	SLC38A4	solute carrier family 38, member 4
28	2,0214	PCDHB6	protocadherin beta 6
29	2,0134	DNAJC27	DnaJ (Hsp40) homolog, subfamily C, member 27
30	2,0054	TNFRSF10C	tumor necrosis factor receptor superfamily, member 10c, decoy without an intracellular domain
31	1,9988	CSRP2	cysteine and glycine-rich protein 2
32	1,9851	SLC40A1	solute carrier family 40 (iron-regulated transporter), member 1
33	1,9801	CDK1	cyclin-dependent kinase 1
34	1,9789	LDB2	LIM domain binding 2
35	1,9701	MSR1	macrophage scavenger receptor 1
36	1,9510	RHCE	Rh blood group, CcEe antigens
37	1,9367	FAM13C	family with sequence similarity 13, member C
38	1,9290	PIR	pirin (iron-binding nuclear protein)
39	1,9277	COL5A2	collagen, type V, alpha 2
40	1,9256	CKAP2	cytoskeleton associated protein 2
41	1,9109	PIM1	pim-1 oncogene
42	1,9065	PDE11A	phosphodiesterase 11A
43	1,8993	OMD	osteomodulin
44	1,8989	ST6GALNAC5	ST6 (α-N-acetyl-neuraminyl-2,3-β-galactosyl-1,3)-N-acetylgalactosaminide α-2,6-sialyltransferase 5
45	1,8947	ZNF506	zinc finger protein 506
46	1,8918	AP4E1	adaptor-related protein complex 4, epsilon 1 subunit
47	1,8907	SFRP2	secreted frizzled-related protein 2
48	1,8823	MESDC2	mesoderm development candidate 2
49	1,8808	LIN7A	lin-7 homolog A (C. elegans)
50	1,8749	MTR	5-methyltetrahydrofolate-homocysteine methyltransferase

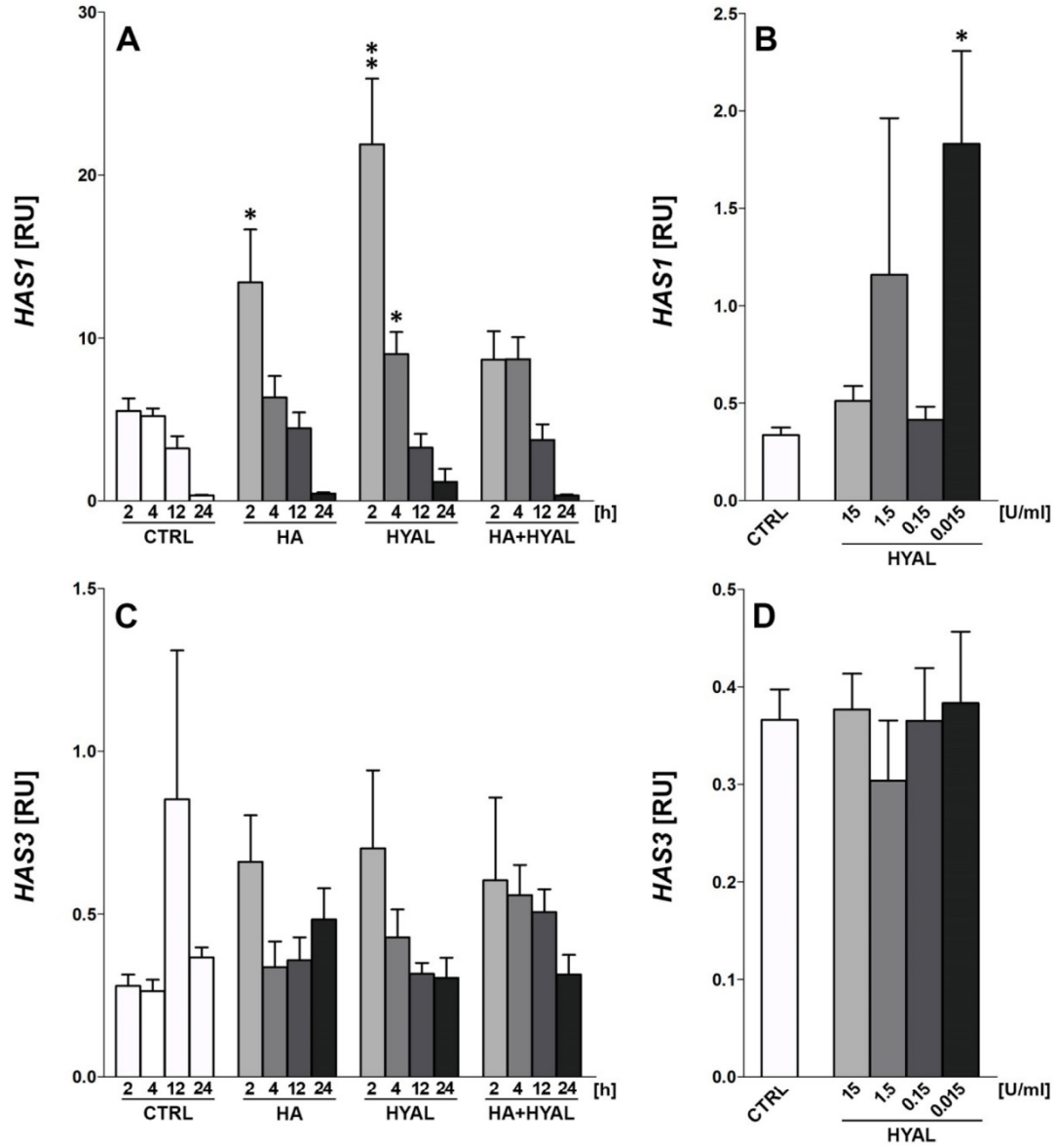

Figure S1. (A, C) HAS1, HAS3 gene expression levels in normal human dermal fibroblasts (NHDF) after stimulation with 1 mg/ml HA, 1.5 U/ml HYAL and HA+HYAL co-stimulation for 2 h, 4 h, 12 h and 24 h, (B, D) HAS1, HAS3 gene expression levels of NHDF after stimulation with 15 U/ml, 1.5 U/ml, 0.15 U/ml and 0.015 U/ml HYAL for 24 h. Asterisks above columns indicate statistical significant differences compared to their respective medium controls. *p ≤ 0.05, **p ≤ 0.01, ***p ≤ 0.001 (t-test, two-sided).

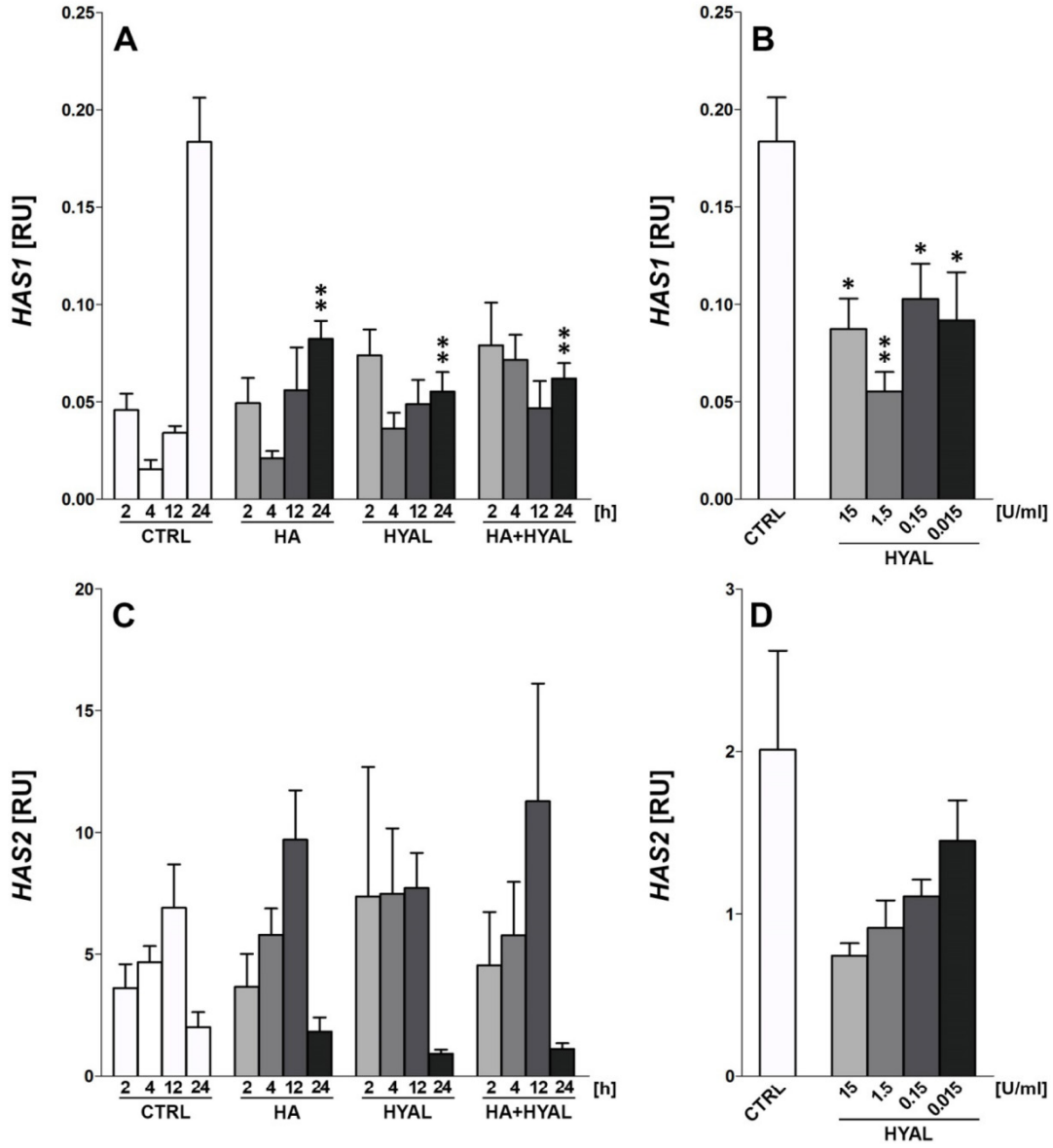
A
B
C
D
HAS1 [RU]
HAS2 [RU]
0.25
0.20
0.15
0.10
0.05
0.00
20
15
10
5
0
3
2
1
2 4 12 24
CTRL
HA
HYAL
HA+HYAL
[h]
15
1.5
0.15
0.015
[U/ml]
*
**

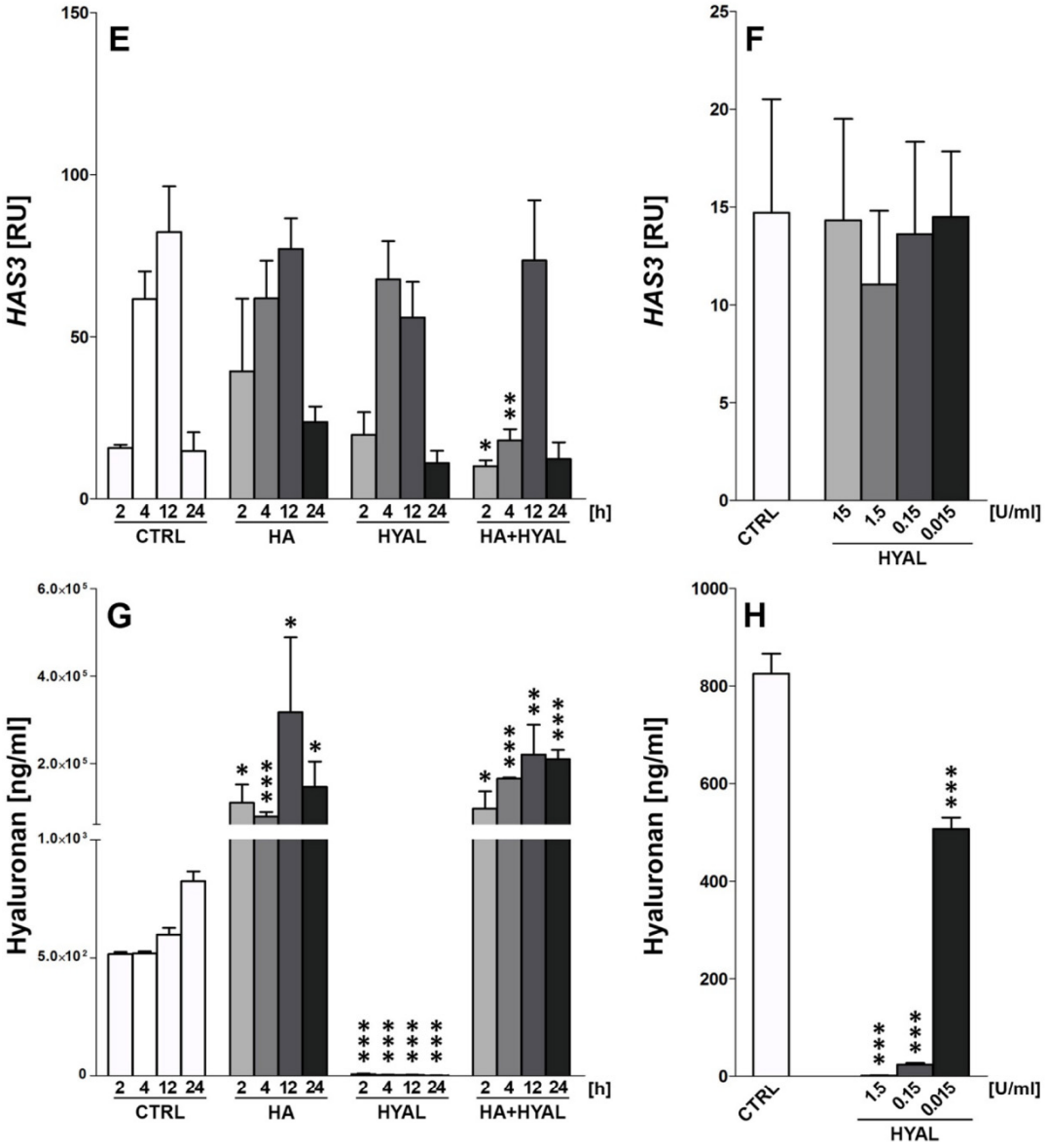

Figure S2. (A, C, E) HAS1, HAS2, HAS3 gene expression levels in primary human keratinocytes after stimulation with 1 mg/ml HA, 1.5 U/ml HYAL and HA+HYAL co-stimulation for 2 h, 4 h, 12 h and 24 h, (B, D, F) HAS1, HAS2, HAS3 gene expression levels in keratinocytes after stimulation with 15 U/ml, 1.5 U/ml, 0.15 U/ml and 0.015 U/ml HYAL for 24 h, (G, H) HA amount (ng/ml) measurement by means of ELISA in supernatants of NHDF treated as described in A-F. Asterisks above columns indicate statistical significant differences compared to their respective medium controls. *p ≤ 0.05, **p ≤ 0.01, ***p ≤ 0.001 (t-test, two-sided).

3. Discussion

The effects of HA and HYAL on structural cells in normal human skin have not been clarified in detail, yet. In this thesis, new insights in HA metabolism have been gained by means of comprehensive genome-wide Affymetrix GeneChip® expression analyses followed by qPCR validation and quantitative protein analyses.

Comprehensive literature search suggests an important role of structural skin cells such as dermal fibroblasts but also epidermal keratinocytes in HA metabolism. For instance, a wide variety of chemical signals have been found to stimulate HA biosynthesis such as cytokines like transforming growth factor-β (Midgley et al., 2013, Sugiyama et al., 1998) or interferon-γ (Sayo et al., 2002), different growth factors like epidermal growth factor (Jeon et al., 2019, Rock et al., 2012) or keratinocyte growth factor (Karvinen et al., 2003), but also retinoic acid (Saavalainen et al., 2005) as well as enzymatic degradation (Larnier et al., 1989). However, regulatory mechanisms of HA synthesis remain elusive.

In this thesis, initial Affymetrix GeneChip® expression analyses were carried out to systematically investigate the effects of HA and HYAL in NHDF. Consecutively, in comprehensive bioinformatic analyses, gene lists were generated containing the 50 most upregulated and most downregulated genes (Tables S1 – S6). Following 24 hours (h) stimulation of NHDF with bovine HYAL, induction of different genes within the late cornified envelope gene cluster (LCE2A, LCE2C, LCE3A, LCE1F) could be observed. These genes which encode major proteins of late epidermal differentiation are located on human chromosome 1q21 and belong to the “epidermal differentiation complex” (EDC) (Kypriotou et al., 2012, Mischke et al., 1996). LCE genes are attributed to skin barrier function and respond to environmental stimuli such as changes in calcium levels and UVB irradiation (Bergboer et al., 2011, Jackson et al., 2005).

The list of top 50 induced genes also includes candidates which are involved in tissue repair and regeneration such as matrix metalloproteinases (MMPs) but also comprises ligands of the epidermal growth factor receptor (EGFR) signaling pathway like heparin-binding EGF-like growth factor (HBEGF) and transforming growth factor alpha (TGFA). MMP-10 or stromelysin-2 (fold change 2.02, rank 20, Table S1) is able to degrade several collagens and non-collagenous connective

tissue substrates including proteoglycans, and is found to be induced at the leading edge of the wounding site in response to skin injury (Caley et al., 2015, Vaalamo et al., 1996). The epidermal growth factor (EGF) family members HBEGF (fold change 1.98, rank 26, Table S1) and TGFA (fold change 1.93, rank 20, Table S1) are critical regulators of migration, proliferation and differentiation of many cell types involved in wound healing and are each capable of stimulating HA synthesis (Bachem et al., 1989, Pasonen-Seppanen et al., 2008). Interestingly, EGFR knockout mice showed striking abnormalities such as wavy hair and deficient skin barrier function (Buhren, 2009, Lichtenberger et al., 2013, Shirakata et al., 2005). Shirakata et al. found that HBEGF is induced in wound healing predominantly at the migrating epidermal edge and functions by accelerating migration responses of human keratinocytes (Shirakata et al., 2005). HBEGF as an EGFR ligand is also required to mediate wound healing associated synthesis of HA and epithelial-mesenchymal transition (Monslow et al., 2009, Stoll et al., 2012). In contrast, neutralization of HBEGF results in diminished accumulation of HA after tissue injury (Dao et al., 2018).

Additionally, interleukin-8 (IL-8; fold change 1.83, rank 50, Table S1) is well known to be expressed by numerous cells including fibroblasts (Strieter et al., 1989) and keratinocytes (Kondo et al., 1993). It plays a pivotal role in neutrophil recruitment and degranulation (Taub et al., 1996) and is also known to induce keratinocyte migration and proliferation, and enhanced re-epithelialization (Baggiolini et al., 1989, Rennekampff et al., 2000).

Finally, the HA synthase HAS3 (fold change 1.80, rank 58, data not shown) showed an induced expression after HYAL stimulation in NHDF. Interestingly, in HYAL-treated NHDF the mRNA transcription levels of the HA synthase isoforms HAS1 and HAS2 are also increased.

Thus, in summary, there is a relevant set of gene candidates each strongly and positively associated with wound healing and tissue remodeling.

In line with these findings, published data suggests that enzymatic degradation of HA but also HA itself can stimulate HA induction in *in vitro* cell culture systems. The working group of Larnier et al. analyzed the effects of bovine testicular HYAL treatment on the incorporation of [^{3}H]-glucosamine into HA in human skin fibroblast cultures. They found that the enzymatic degradation of HA by HYAL induced a specific stimulation of HA synthesis which resulted in an increase in

the amount of newly synthesized HA secreted into the medium (Larnier et al., 1989, Moczar and Robert, 1993). Equivalently, results in this thesis show that treatment with HYAL increases HA amounts in conditioned supernatants of NHDF as measured by ELISA. Of interest, elevated HA amounts were especially found in the medium of those cells which showed high mRNA expression of the HA synthase HAS2 but no other isoforms.

A wide variety of studies showed that HAS2 is the major isoform responsible for HA synthesis in fibroblastic cells (Sapudom et al., 2020). HAS2 is the only gene which knockout deletion ($Has2^{-/-}$ mice) leads to embryonic lethality at day 9.5 due to a failure to form HA-rich organs. Those mice exhibit severe cardiac and vascular deficiencies. Interestingly, administering of exogenous HA or restoring gene function in $Has2^{-/-}$ explants could rescue abnormalities (Camenisch et al., 2002, Camenisch et al., 2000, Passi et al., 2019). Moreover, Röck et al. found that HAS2 appeared to be the most abundant isoform in skin fibroblasts as the extent of HAS2 downregulation correlated with the decrease of HA secretion (Rock et al., 2011). Data therefore highlights the predominant role of HAS2 in the regulation of HA and reveals its important role for HA metabolism.

However, the increase of HA amount in the supernatants of HYAL-treated NHDF might be explained as a potential compensatory mechanism of transient HYAL-induced HA loss in fibroblasts (Fig. 3). As a consequence, HA synthesis might be induced and therefore compensate HYAL-mediated degradation of HA locally. Another possible explanation could be the passive clearing of membrane-bound HA into the medium. Since radioactive HA labeling and HYAL activity studies were not included in this thesis, these specific questions could be addressed in future experiments.

In this thesis dose-titration experiments were performed. Here, NHDF were treated with decreasing doses of HYAL. Unexpectedly, HAS2 mRNA gene expression increased with decreasing concentration of HYAL. Interestingly, the strongest induction of HAS2 could be observed in cells when HYAL was used at its lowest concentration (0.015 U/ml). Analogously, the highest amount of newly synthesized HA was measured in supernatants of those cells treated with the lowest concentration of HYAL.

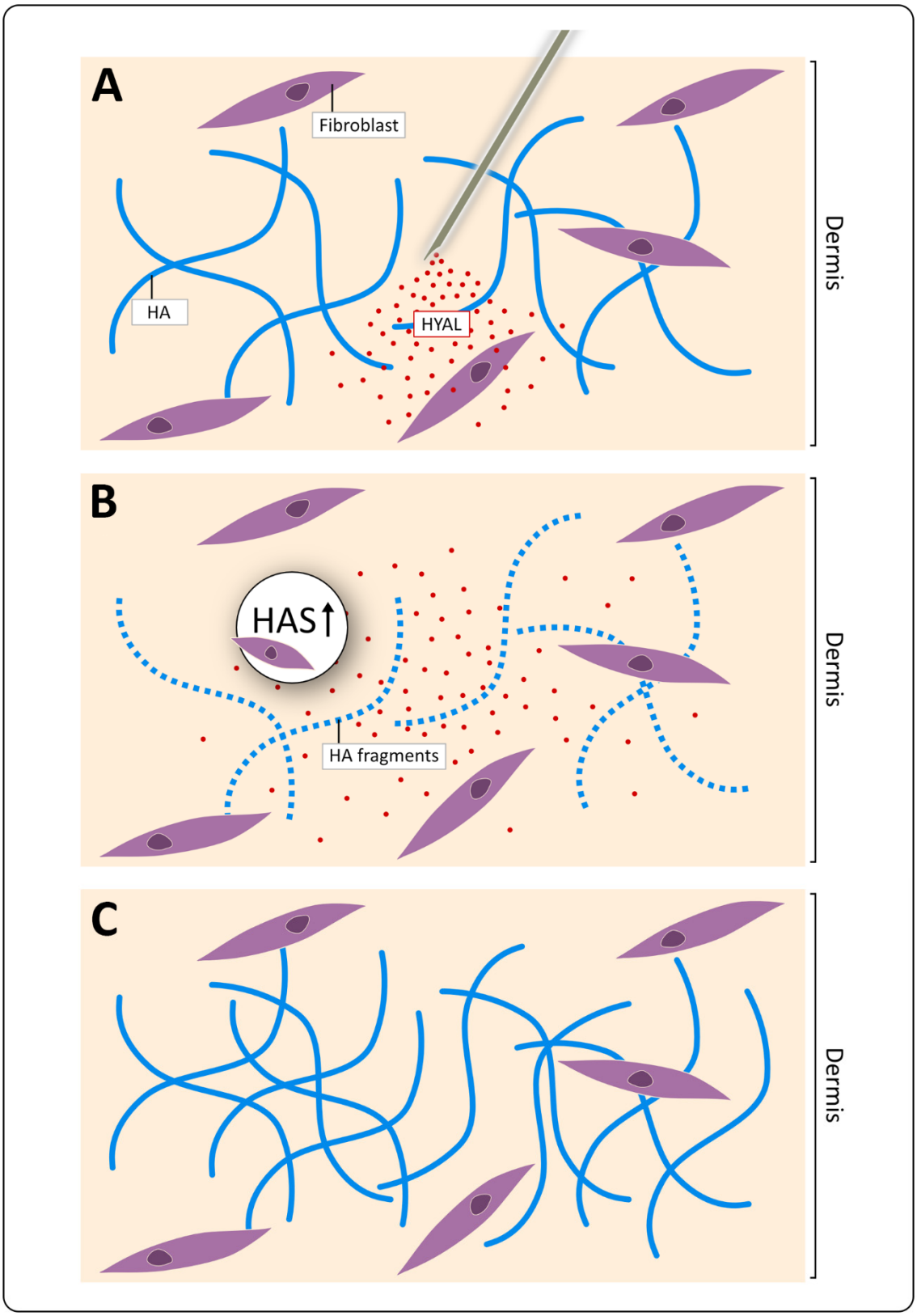

Fig. 3 Putative role of HYAL in HA metabolism. (A) The injection of low-dose HYAL into the skin depolymerizes HA into smaller fragments. **(B)** HYAL and HYAL-mediated breakdown products induce the upregulation of HA synthase genes such as HAS2. **(C)** The induction of HA synthesis leads to an accumulation of HA compensating the HYAL-mediated degradation of HA locally. Modified after: Buhren et al., 2020

Finally, in *ex vivo* human skin samples incubated with HYAL, quantitative immunohistochemical analyses revealed similar observations: whereas the application of low dose HYAL (0.015 U/ml) led to a pronounced accumulation of HA, high concentrations of HYAL (15 U/ml) reduced the level of measured dermal HA. Correspondingly, the working group of Philipson et al. (Philipson et al., 1985) could show that low dose HYAL treatment of cells in a monolayer culture caused a 4- to 5-fold stimulation of HA activity not only in cultured cells but also in isolated membrane preparations (Philipson and Schwartz, 1984) which suggests the presence of a feedback mechanism enabling cells to sense levels of HA that has been synthesized (Stern, 2003, Stern, 2004). After HA is synthesized at the inner side of the plasma membrane, it is extruded to the cell surface where it can be degraded extracellularly by exogenously added HYAL (Prehm, 1984). Consequently, the transient hyaluronidase degradation of HA which translates that only insufficient quantities of HA have been synthesized might in turn result in an induction of HA synthesis to compensate HA deficits (Stern, 2003). An ever increasing number of evidences suggest the existence of a putative mini-organelle lying just under and partially embedded within the plasma membrane that is responsible for such a feedback mechanism (Stern, 2004). This putative multi-protein membrane associated complex containing both synthetic and catabolic activities might provide sensitive sensor mechanisms to respond dynamically to a variety of metabolic states (Stern, 2010). Decades ago, the working group of Mian et al. characterized a high-M_r plasma-membrane-bound protein as a constituent of HA synthase complex featuring catabolic activity that was purified from human skin fibroblasts (Mian, 1986b, Mian, 1986a). On the basis of parallels to glycogen granules which occur in muscle and liver tissue, some years later Robert Stern proposed a name for this mini-organelle – the hyaluronasome (Stern, 2003, Stern, 2010). Also still speculative, Robert Stern suggested that the hyaluronasome might be a membrane-bound structure which can respond dynamically to extracellular events but also intracellular metabolic states of the cell to regulate levels of HA deposition with great precision (Stern, 2003, Stern, 2004). When the HA polymer after it is being extruded into the extracellular space is constantly clipped and degraded by HYAL this “misinformation” that only insufficient HA has been generated could in turn stimulate HA synthesis in a positive feedback loop (Fig. 3). Therefore, the

existence of such a multiplayer like the hyaluronasome could explain observations that low dose treatment of HYAL rather leads to induction of HA-metabolism as compared to higher concentrations of HYAL which will lead to a total breakdown of all available HA as could be demonstrated in this thesis' ELISA experiments. Still to be elucidated, in order to provide the structural organization, the hyaluronasome could work as a functional unit containing a variety of tools such as the HA receptors RHAMM and CD44, the HA synthase enzymes HAS1, HAS2, HAS3, the hyaluronidases, the hyaluronidase inhibitors, and hyaluronan binding protein 1 (HABP1) (Stern, 2003). Especially, the HA receptor CD44 which is plasma membrane bound seems to be an ideal candidate involved in a potential feedback mechanism described above. Of interest, it has already been shown that the expression of CD44 alternative splicing isoforms can be modulated in response to HYAL treatment (Stern et al., 2001, Tanabe et al., 1993). In addition, Dowthwaite et al. could show that the decrease in liberated HA by HYAL treatment in fibrocartilage cells not only significantly increased the release of HA into tissue culture media over 24 h but was also associated with an increased CD44 expression, induction of HA synthase gene expression, and an enhanced binding of HA to the cell surface (Dowthwaite et al., 2003). In order to proof the existence of such a mini-organelle which (i) instructs the cell on how much HA has been made and (ii) which can respond dynamically to synthesize the needed amount of HA, cellular signal transduction analyses and immunohistochemical colocalization studies are still required to allow mechanistic insights.

As demonstrated above, there is a dynamic feedback mechanism between HA synthesis and degradation which regulates the net deposition of HA in the cell. Out of a variety of cells from fibroblastic and epithelial origin, dermal human fibroblasts exhibit highest HA synthesizing activity (Li et al., 2007). Published data as well as results presented in this thesis indicate that HAS3 plays a crucial role in regulation of HA synthesis within the epidermis as demonstrated in cultured keratinocytes (Malaisse et al., 2014, Sayo et al., 2002), while HAS2 produces HA in fibroblasts (Rock et al., 2011, Sapudom et al., 2020, Yamada et al., 2004). In addition, in NHDF the overall basal HA production was stronger as compared to HEK.

Until now, effects of HA and HYAL on re-epithelialization of wounds are not yet fully understood. Wound healing is comprised of complex, sequential and dynamic processes that can be divided into four distinct phases overlapping in time and space: (i) haemostasis, (ii) inflammation, (iii) proliferation, and (iv) remodeling (Ghatak et al., 2015). Firstly, at the site of injury vascular constriction and platelet aggregation trigger the formation of a temporary fibrin clot which provides a provisional matrix for migrating cells (Maytin, 2016). Adherence of platelets to the injured endothelium, coagulation, and the activated-complement pathways lead to the release of chemokines and numerous vasoactive mediators thereby recruiting a variety of cells of the inflammatory phase (DiPietro et al., 1998, Gosain and DiPietro, 2004, Singer and Clark, 1999). Once the leakage from damaged blood vessels is controlled, inflammatory cells such as neutrophils, macrophages, and lymphocytes sequentially infiltrate into the wound attracted by chemotaxis (Ghatak et al., 2015). Following clearance of invading pathogens and cellular debris, neutrophils are phagocytosed by macrophages which help the resolution of inflammation (Ghatak et al., 2015). The third phase is characterized by rapid cellular migration and proliferation leading to the formation of a newly synthesized ECM – the granulation tissue (Velnar et al., 2009). Thereafter, the phase of remodeling takes several months which results in increased wound strength and scar tissue formation (Maytin, 2016). Although it has been well established that HA is associated with tissue repair, it appears to have distinct biological effector functions depending on the basis of its molecular weight and depending on the circumstances under which it is produced (Chen and Abatangelo, 1999, Noble, 2002). Immediately after skin injury an accumulation of especially HMW-HA occurs in the ECM which is fundamental for clot formation (D'Agostino et al., 2015). Thereafter, in the inflammatory phase of wound healing, particularly LMW-HA can be found in the wounding bed which partly results from HMW-HA breakdown due to the rising levels of HYAL which is produced in the wound (D'Agostino et al., 2015, Maharjan et al., 2011, Noble, 2002). The major function of these HA fragments includes the modulation of inflammatory and fibroblast cell migration, synthesis of proinflammatory chemokines, and activation of macrophages for phagocytosis (Chen and Abatangelo, 1999, D'Agostino et al., 2015, Ghatak et al., 2015, Stern et al., 2006).

Evidence from fundamental literature suggests a beneficial role of exogenously applied HA for cutaneous tissue repair (Aya and Stern, 2014, D'Agostino et al., 2015, Diegelmann and Evans, 2004, Galeano et al., 2011, Prosdocimi and Bevilacqua, 2012). In this thesis' wound healing assay, which was performed on a monolayer of scratched dermal fibroblasts, treatment with HA resulted in faster wound healing as compared to medium controls. Of interest, treatment with HYAL enhanced wound closure rate to the same extend. Interestingly, acceleration of cutaneous wound healing in the presence of HYAL has also been described by Fronza et al. in an *in vivo* full thickness excision wound model in Wistar rats (Fronza et al., 2014). Depending on the stage of wound healing they found an increased migration and proliferation of fibroblasts, induction of proinflammatory cytokines, a robust increase in the organization of collagen fibers, and an augmentation in angiogenesis (Fronza et al., 2014). Especially LMW-HA has been suggested to play a pivotal role in tissue repair (West et al., 1985). As HYAL is able to depolymerize HA, it might contribute to the balance between HA synthesis und HA fragmentation. Size specific degradation products of HA might then be beneficial as healing promoting agents for cutaneous injuries (Fronza et al., 2014).

Decreased wound healing capacity in the aging skin is attributed in part to age-dependent changes in HA metabolism such as decreased ability to process HA (Meyer and Stern, 1994, Stern and Maibach, 2008). Similarly, in the wounded skin of aged mice Reed et al. found decreased levels of LMW-HA in comparison to the dermis of young mice (Reed et al., 2013). The lack to generate such small fragments either due to reduced HYAL expression in the aged wound dermis (Reed et al., 2013) or due to an inability to synthesize smaller fragments would then compromise the healing process. In the aging human skin, the use of HA fillers for soft tissue augmentation has become increasingly popular due to its efficiency and safety since excessed material can be removed with the help of HYAL (Buhren et al., 2018, Buhren et al., 2016). Whether the improved appearance of skin is accompanied by the passive augmentation of physical volume or other mechanisms which include remodeling of the ECM is elusive. The study group of Wang et al. examined photodamaged skin biopsies of healthy volunteers after dermal HA filler injections and found a *de novo* synthesis of type I collagen which they attributed to mechanical stretching and consequent

activation of collagen-producing fibroblasts in the dermis (Wang et al., 2007). Later on, the laboratory of Voorhees and Fisher showed that the injection of a cross-linked HA (Restylane®) into aged skin stimulated localized proliferation of fibroblasts and increased epidermal thickness (Quan et al., 2013). Examined fibroblasts were associated with type I collagen synthesis and exhibited an elongated stretched morphology resembling those in healthy young skin, suggesting that functional capacity in the aging skin can be partially restored (Fisher et al., 2016, Roy et al., 2020, Quan et al., 2013). However, it is to consider that the activation of ECM producing cells might be the result of different possibilities such as direct binding of HA fillers to cellular receptors, mechanical forces, or the result of low-level inflammation induced by the HA filler itself leading to fragmentation of HA (Quan et al., 2013). Thus, the increased concentration of HA fragments might then be beneficial in the rejuvenation of aged skin as it stimulates dermal fibroblasts to increase products of the ECM such as collagen and HA thereby restoring components which have been lost in photoaging. In this thesis, the external application of low-dose HYAL might utilize similar effects as it can elevate available amounts of fragmented HA via enzymatic degradation of HA which in turn might stimulate functional activation of fibroblasts. However, the dose-dependent application of small HA fragment sizes was not investigated in our study which could be addressed in future studies.

In conclusion, the endoglucosaminidase HYAL is a bioactive enzyme that can exert a wide variety of effects on the HA metabolism in structural cells of the skin. Evidently, in this thesis it was demonstrated that especially low concentrations of HYAL resulted in a significant induction not only of HAS genes but also in an all over HA accumulation. In contrast, higher concentrations of HYAL downmodulated the amount of HA. Therefore, results of this thesis indicate that low-dose HYAL treatment might be involved in activating dermal fibroblasts to stimulate HA synthesis. Additionally, findings of this thesis point toward an important role of HYAL in wound healing as HYAL accelerates wound closure in an *in vitro* wound scratch model of dermal fibroblasts. Nevertheless, future experiments aiming to unravel the underlying mechanisms of HA and HYAL biology are necessary for potential medical applications not only for dermatologists but also for other clinicians as well.

4. References

ABDO, J. M., SOPKO, N. A. & MILNER, S. M. 2020. The applied anatomy of human skin: A model for regeneration. *Wound Medicine,* 28**,** 100179.

ADAMIA, S., MAXWELL, C. A. & PILARSKI, L. M. 2005. Hyaluronan and hyaluronan synthases: potential therapeutic targets in cancer. *Curr Drug Targets Cardiovasc Haematol Disord,* 5**,** 3-14.

ADAMIA, S., PILARSKI, P. M., BELCH, A. R. & PILARSKI, L. M. 2013. Aberrant splicing, hyaluronan synthases and intracellular hyaluronan as drivers of oncogenesis and potential drug targets. *Curr Cancer Drug Targets,* 13**,** 347-61.

AYA, K. L. & STERN, R. 2014. Hyaluronan in wound healing: rediscovering a major player. *Wound Repair Regen,* 22**,** 579-93.

BACHEM, M. G., RIESS, U., MELCHIOR, R., SELL, K. M. & GRESSNER, A. M. 1989. Transforming growth factors (TGF alpha and TGF beta 1) stimulate chondroitin sulfate and hyaluronate synthesis in cultured rat liver fat storing cells. *FEBS Lett,* 257**,** 134-7.

BAGGIOLINI, M., WALZ, A. & KUNKEL, S. L. 1989. Neutrophil-activating peptide-1/interleukin 8, a novel cytokine that activates neutrophils. *J Clin Invest,* 84**,** 1045-9.

BAILEY, S. H., FAGIEN, S. & ROHRICH, R. J. 2014. Changing role of hyaluronidase in plastic surgery. *Plast Reconstr Surg,* 133**,** 127e-132e.

BELLIN, M. F., JAKOBSEN, J. A., TOMASSIN, I., THOMSEN, H. S., MORCOS, S. K., THOMSEN, H. S., MORCOS, S. K., ALMEN, T., ASPELIN, P., BELLIN, M. F., CLAUSS, W., FLATEN, H., GRENIER, N., IDEE, J. M., JAKOBSEN, J. A., KRESTIN, G. P., STACUL, F., WEBB, J. A. & CONTRAST MEDIA SAFETY COMMITTEE OF THE EUROPEAN SOCIETY OF UROGENITAL, R. 2002. Contrast medium extravasation injury: guidelines for prevention and management. *Eur Radiol,* 12**,** 2807-12.

BERGBOER, J. G., TJABRINGA, G. S., KAMSTEEG, M., VAN VLIJMEN-WILLEMS, I. M., RODIJK-OLTHUIS, D., JANSEN, P. A., THURET, J. Y., NARITA, M., ISHIDA-YAMAMOTO, A., ZEEUWEN, P. L. & SCHALKWIJK, J. 2011. Psoriasis risk genes of the late cornified envelope-3 group are distinctly expressed compared with genes of other LCE groups. *Am J Pathol,* 178**,** 1470-7.

BOHAUMILITZKY, L., HUBER, A. K., STORK, E. M., WENGERT, S., WOELFL, F. & BOEHM, H. 2017. A Trickster in Disguise: Hyaluronan's Ambivalent Roles in the Matrix. *Front Oncol,* 7**,** 242.

BONNANS, C., CHOU, J. & WERB, Z. 2014. Remodelling the extracellular matrix in development and disease. *Nat Rev Mol Cell Biol,* 15**,** 786-801.

BOULAIS, N. & MISERY, L. 2008. The epidermis: a sensory tissue. *Eur J Dermatol,* 18**,** 119-27.

BRACKE, K. R., DENTENER, M. A., PAPAKONSTANTINOU, E., VERNOOY, J. H., DEMOOR, T., PAUWELS, N. S., CLEUTJENS, J., VAN SUYLEN, R. J., JOOS, G. F., BRUSSELLE, G. G. & WOUTERS, E. F. 2010. Enhanced deposition of low-molecular-weight hyaluronan in lungs of cigarette smoke-exposed mice. *Am J Respir Cell Mol Biol,* 42**,** 753-61.

BUHREN, B. A. 2009. *Unraveling the mechanisms of EGFR-inhibitor associated cutaneous adverse effects,* Duesseldorf, Heinrich-Heine-University, Dissertation, https://docserv.uni-duesseldorf.de/servlets/DerivateServlet/Derivate-15851/BuhrenBA%20PhD%20Thesis.pdf.

BUHREN, B. A., SCHRUMPF, H., BOLKE, E., KAMMERS, K. & GERBER, P. A. 2018. Standardized in vitro analysis of the degradability of hyaluronic acid fillers by hyaluronidase. *Eur J Med Res,* 23**,** 37.

BUHREN, B. A., SCHRUMPF, H., GORGES, K., REINERS, O., BOLKE, E., FISCHER, J. W., HOMEY, B. & GERBER, P. A. 2020. Dose- and time-dependent effects of hyaluronidase on structural cells and the extracellular matrix of the skin. *Eur J Med Res,* 25**,** 60.

BUHREN, B. A., SCHRUMPF, H., HOFF, N. P., BOLKE, E., HILTON, S. & GERBER, P. A. 2016. Hyaluronidase: from clinical applications to molecular and cellular mechanisms. *Eur J Med Res,* 21**,** 5.

CALEY, M. P., MARTINS, V. L. & O'TOOLE, E. A. 2015. Metalloproteinases and Wound Healing. *Adv Wound Care (New Rochelle),* 4**,** 225-234.

CAMENISCH, T. D., SCHROEDER, J. A., BRADLEY, J., KLEWER, S. E. & MCDONALD, J. A. 2002. Heart-valve mesenchyme formation is dependent on hyaluronan-augmented activation of ErbB2-ErbB3 receptors. *Nat Med,* 8**,** 850-5.

CAMENISCH, T. D., SPICER, A. P., BREHM-GIBSON, T., BIESTERFELDT, J., AUGUSTINE, M. L., CALABRO, A., JR., KUBALAK, S., KLEWER, S. E. & MCDONALD, J. A. 2000. Disruption of hyaluronan synthase-2 abrogates normal cardiac morphogenesis and hyaluronan-mediated transformation of epithelium to mesenchyme. *J Clin Invest,* 106**,** 349-60.

CHEN, W. Y. & ABATANGELO, G. 1999. Functions of hyaluronan in wound repair. *Wound Repair Regen,* 7**,** 79-89.

CONSTANS, T., DUTERTRE, J. P. & FROGE, E. 1991. Hypodermoclysis in dehydrated elderly patients: local effects with and without hyaluronidase. *J Palliat Care,* 7**,** 10-2.

CSOKA, A. B., FROST, G. I. & STERN, R. 2001. The six hyaluronidase-like genes in the human and mouse genomes. *Matrix Biol,* 20**,** 499-508.

CYPHERT, J. M., TREMPUS, C. S. & GARANTZIOTIS, S. 2015. Size Matters: Molecular Weight Specificity of Hyaluronan Effects in Cell Biology. *Int J Cell Biol,* 2015**,** 563818.

D'AGOSTINO, A., STELLAVATO, A., BUSICO, T., PAPA, A., TIRINO, V., PAPACCIO, G., LA GATTA, A., DE ROSA, M. & SCHIRALDI, C. 2015. In vitro analysis of the effects on wound healing of high- and low-molecular weight chains of hyaluronan and their hybrid H-HA/L-HA complexes. *BMC Cell Biol,* 16**,** 19.

DAO, D. T., ANEZ-BUSTILLOS, L., ADAM, R. M., PUDER, M. & BIELENBERG, D. R. 2018. Heparin-Binding Epidermal Growth Factor-Like Growth Factor as a Critical Mediator of Tissue Repair and Regeneration. *Am J Pathol,* 188**,** 2446-2456.

DE OLIVEIRA, J. D., CARVALHO, L. S., GOMES, A. M., QUEIROZ, L. R., MAGALHAES, B. S. & PARACHIN, N. S. 2016. Genetic basis for hyper production of hyaluronic acid in natural and engineered microorganisms. *Microb Cell Fact,* 15**,** 119.

DIEGELMANN, R. F. & EVANS, M. C. 2004. Wound healing: an overview of acute, fibrotic and delayed healing. *Front Biosci,* 9**,** 283-9.

DIPIETRO, L. A., BURDICK, M., LOW, Q. E., KUNKEL, S. L. & STRIETER, R. M. 1998. MIP-1alpha as a critical macrophage chemoattractant in murine wound repair. *J Clin Invest,* 101**,** 1693-8.

DOWTHWAITE, G. P., FLANNERY, C. R., FLANNELLY, J., LEWTHWAITE, J. C., ARCHER, C. W. & PITSILLIDES, A. A. 2003. A mechanism underlying the movement requirement for synovial joint cavitation. *Matrix Biol,* 22**,** 311-22.

FALLACARA, A., BALDINI, E., MANFREDINI, S. & VERTUANI, S. 2018. Hyaluronic Acid in the Third Millennium. *Polymers (Basel),* 10.

FISHER, G. J., SHAO, Y., HE, T., QIN, Z., PERRY, D., VOORHEES, J. J. & QUAN, T. 2016. Reduction of fibroblast size/mechanical force down-regulates TGF-beta type II receptor: implications for human skin aging. *Aging Cell,* 15**,** 67-76.

FRANTZ, C., STEWART, K. M. & WEAVER, V. M. 2010. The extracellular matrix at a glance. *J Cell Sci,* 123**,** 4195-200.

FRONZA, M., CAETANO, G. F., LEITE, M. N., BITENCOURT, C. S., PAULA-SILVA, F. W., ANDRADE, T. A., FRADE, M. A., MERFORT, I. & FACCIOLI, L. H. 2014.

Hyaluronidase modulates inflammatory response and accelerates the cutaneous wound healing. *PLoS One,* 9**,** e112297.

GALEANO, M., POLITO, F., BITTO, A., IRRERA, N., CAMPO, G. M., AVENOSO, A., CALO, M., LO CASCIO, P., MINUTOLI, L., BARONE, M., SQUADRITO, F. & ALTAVILLA, D. 2011. Systemic administration of high-molecular weight hyaluronan stimulates wound healing in genetically diabetic mice. *Biochim Biophys Acta,* 1812**,** 752-9.

GERBER, P. A., BUHREN, B. A., SCHRUMPF, H., HOMEY, B., ZLOTNIK, A. & HEVEZI, P. 2014. The top skin-associated genes: a comparative analysis of human and mouse skin transcriptomes. *Biol Chem,* 395**,** 577-91.

GHATAK, S., MAYTIN, E. V., MACK, J. A., HASCALL, V. C., ATANELISHVILI, I., MORENO RODRIGUEZ, R., MARKWALD, R. R. & MISRA, S. 2015. Roles of Proteoglycans and Glycosaminoglycans in Wound Healing and Fibrosis. *Int J Cell Biol,* 2015**,** 834893.

GIRISH, K. S. & KEMPARAJU, K. 2007. The magic glue hyaluronan and its eraser hyaluronidase: a biological overview. *Life Sci,* 80**,** 1921-43.

GOSAIN, A. & DIPIETRO, L. A. 2004. Aging and wound healing. *World J Surg,* 28**,** 321-6.

HELDIN, P., LIN, C. Y., KOLLIOPOULOS, C., CHEN, Y. H. & SKANDALIS, S. S. 2019. Regulation of hyaluronan biosynthesis and clinical impact of excessive hyaluronan production. *Matrix Biol,* 78-79**,** 100-117.

IOZZO, R. V., ZOELLER, J. J. & NYSTROM, A. 2009. Basement membrane proteoglycans: modulators Par Excellence of cancer growth and angiogenesis. *Mol Cells,* 27**,** 503-13.

ITANO, N. & KIMATA, K. 2002. Mammalian hyaluronan synthases. *IUBMB Life,* 54**,** 195-9.

ITANO, N., SAWAI, T., YOSHIDA, M., LENAS, P., YAMADA, Y., IMAGAWA, M., SHINOMURA, T., HAMAGUCHI, M., YOSHIDA, Y., OHNUKI, Y., MIYAUCHI, S., SPICER, A. P., MCDONALD, J. A. & KIMATA, K. 1999. Three isoforms of mammalian hyaluronan synthases have distinct enzymatic properties. *J Biol Chem,* 274**,** 25085-92.

JACKSON, B., TILLI, C. M., HARDMAN, M. J., AVILION, A. A., MACLEOD, M. C., ASHCROFT, G. S. & BYRNE, C. 2005. Late cornified envelope family in differentiating epithelia--response to calcium and ultraviolet irradiation. *J Invest Dermatol,* 124**,** 1062-70.

JEON, Y. J., KIM, Y. H., JEON, Y. J., LEE, W. W., BAE, I. G., YI, K. W. & HONG, S. H. 2019. Increased synthesis of hyaluronic acid by enhanced penetration of CTP-EGF recombinant in human keratinocytes. *J Cosmet Dermatol*.

JUHLIN, L. 1997. Hyaluronan in skin. *J Intern Med,* 242**,** 61-6.

KALLIO, H., PALOHEIMO, M. & MAUNUKSELA, E. L. 2000. Hyaluronidase as an adjuvant in bupivacaine-lidocaine mixture for retrobulbar/peribulbar block. *Anesth Analg,* 91**,** 934-7.

KANITAKIS, J. 2002. Anatomy, histology and immunohistochemistry of normal human skin. *Eur J Dermatol,* 12**,** 390-9; quiz 400-1.

KARVINEN, S., PASONEN-SEPPANEN, S., HYTTINEN, J. M., PIENIMAKI, J. P., TORRONEN, K., JOKELA, T. A., TAMMI, M. I. & TAMMI, R. 2003. Keratinocyte growth factor stimulates migration and hyaluronan synthesis in the epidermis by activation of keratinocyte hyaluronan synthases 2 and 3. *J Biol Chem,* 278**,** 49495-504.

KNOPF-MARQUES, H., PRAVDA, M., WOLFOVA, L., VELEBNY, V., SCHAAF, P., VRANA, N. E. & LAVALLE, P. 2016. Hyaluronic Acid and Its Derivatives in Coating and Delivery Systems: Applications in Tissue Engineering, Regenerative Medicine and Immunomodulation. *Adv Healthc Mater,* 5**,** 2841-2855.

KNUDSON, C. B. & KNUDSON, W. 1993. Hyaluronan-binding proteins in development, tissue homeostasis, and disease. *FASEB J,* 7**,** 1233-41.

KOBAYASHI, T., CHANMEE, T. & ITANO, N. 2020. Hyaluronan: Metabolism and Function. *Biomolecules,* 10.

KONDO, S., KONO, T., SAUDER, D. N. & MCKENZIE, R. C. 1993. IL-8 gene expression and production in human keratinocytes and their modulation by UVB. *J Invest Dermatol,* 101**,** 690-4.

KYPRIOTOU, M., HUBER, M. & HOHL, D. 2012. The human epidermal differentiation complex: cornified envelope precursors, S100 proteins and the 'fused genes' family. *Exp Dermatol,* 21**,** 643-9.

LARNIER, C., KERNEUR, C., ROBERT, L. & MOCZAR, M. 1989. Effect of testicular hyaluronidase on hyaluronate synthesis by human skin fibroblasts in culture. *Biochim Biophys Acta,* 1014**,** 145-52.

LAURENT, T. 1989. The biology of hyaluronan. Introduction. *Ciba Found Symp,* 143**,** 1-20.

LAURENT, T. C. & FRASER, J. R. 1992. Hyaluronan. *FASEB J,* 6**,** 2397-404.

LEE-SAYER, S. S., DONG, Y., ARIF, A. A., OLSSON, M., BROWN, K. L. & JOHNSON, P. 2015. The where, when, how, and why of hyaluronan binding by immune cells. *Front Immunol,* 6**,** 150.

LEE, A., GRUMMER, S. E., KRIEGEL, D. & MARMUR, E. 2010. Hyaluronidase. *Dermatol Surg,* 36**,** 1071-7.

LI, L., ASTERIOU, T., BERNERT, B., HELDIN, C. H. & HELDIN, P. 2007. Growth factor regulation of hyaluronan synthesis and degradation in human dermal fibroblasts: importance of hyaluronan for the mitogenic response of PDGF-BB. *Biochem J,* 404**,** 327-36.

LICHTENBERGER, B. M., GERBER, P. A., HOLCMANN, M., BUHREN, B. A., AMBERG, N., SMOLLE, V., SCHRUMPF, H., BOELKE, E., ANSARI, P., MACKENZIE, C., WOLLENBERG, A., KISLAT, A., FISCHER, J. W., ROCK, K., HARDER, J., SCHRODER, J. M., HOMEY, B. & SIBILIA, M. 2013. Epidermal EGFR controls cutaneous host defense and prevents inflammation. *Sci Transl Med,* 5**,** 199ra111.

MADISON, K. C. 2003. Barrier function of the skin: "la raison d'etre" of the epidermis. *J Invest Dermatol,* 121**,** 231-41.

MAHARJAN, A. S., PILLING, D. & GOMER, R. H. 2011. High and low molecular weight hyaluronic acid differentially regulate human fibrocyte differentiation. *PLoS One,* 6**,** e26078.

MALAISSE, J., BOURGUIGNON, V., DE VUYST, E., LAMBERT DE ROUVROIT, C., NIKKELS, A. F., FLAMION, B. & POUMAY, Y. 2014. Hyaluronan metabolism in human keratinocytes and atopic dermatitis skin is driven by a balance of hyaluronan synthases 1 and 3. *J Invest Dermatol,* 134**,** 2174-2182.

MAYTIN, E. V. 2016. Hyaluronan: More than just a wrinkle filler. *Glycobiology,* 26**,** 553-9.

MEIGEL, W. N., GAY, S. & WEBER, L. 1977. Dermal architecture and collagen type distribution. *Arch Dermatol Res,* 259**,** 1-10.

MEYER, L. J. & STERN, R. 1994. Age-dependent changes of hyaluronan in human skin. *J Invest Dermatol,* 102**,** 385-9.

MIAN, N. 1986a. Analysis of cell-growth-phase-related variations in hyaluronate synthase activity of isolated plasma-membrane fractions of cultured human skin fibroblasts. *Biochem J,* 237**,** 333-42.

MIAN, N. 1986b. Characterization of a high-Mr plasma-membrane-bound protein and assessment of its role as a constituent of hyaluronate synthase complex. *Biochem J,* 237**,** 343-57.

MIDGLEY, A. C., ROGERS, M., HALLETT, M. B., CLAYTON, A., BOWEN, T., PHILLIPS, A. O. & STEADMAN, R. 2013. Transforming growth factor-beta1 (TGF-beta1)-stimulated fibroblast to myofibroblast differentiation is mediated by hyaluronan (HA)-facilitated epidermal growth factor receptor (EGFR) and CD44 co-localization in lipid rafts. *J Biol Chem,* 288**,** 14824-38.

MINE, S., FORTUNEL, N. O., PAGEON, H. & ASSELINEAU, D. 2008. Aging alters functionally human dermal papillary fibroblasts but not reticular fibroblasts: a new view of skin morphogenesis and aging. *PLoS One,* 3**,** e4066.

MISCHKE, D., KORGE, B. P., MARENHOLZ, I., VOLZ, A. & ZIEGLER, A. 1996. Genes encoding structural proteins of epidermal cornification and S100 calcium-binding proteins form a gene complex ("epidermal differentiation complex") on human chromosome 1q21. *J Invest Dermatol,* 106**,** 989-92.

MOCZAR, M. & ROBERT, L. 1993. Stimulation of cell proliferation by hyaluronidase during in vitro aging of human skin fibroblasts. *Exp Gerontol,* 28**,** 59-68.

MONSLOW, J., SATO, N., MACK, J. A. & MAYTIN, E. V. 2009. Wounding-induced synthesis of hyaluronic acid in organotypic epidermal cultures requires the release of heparin-binding egf and activation of the EGFR. *J Invest Dermatol,* 129**,** 2046-58.

MORELAND, L. W. 2003. Intra-articular hyaluronan (hyaluronic acid) and hylans for the treatment of osteoarthritis: mechanisms of action. *Arthritis Res Ther,* 5**,** 54-67.

NESTLE, F. O., DI MEGLIO, P., QIN, J. Z. & NICKOLOFF, B. J. 2009. Skin immune sentinels in health and disease. *Nat Rev Immunol,* 9**,** 679-91.

NEUMAYER, T., PRINZ, A. & FINDL, O. 2008. Effect of a new cohesive ophthalmic viscosurgical device on corneal protection and intraocular pressure in small-incision cataract surgery. *J Cataract Refract Surg,* 34**,** 1362-6.

NOBLE, P. W. 2002. Hyaluronan and its catabolic products in tissue injury and repair. *Matrix Biol,* 21**,** 25-9.

PAPAKONSTANTINOU, E., ROTH, M. & KARAKIULAKIS, G. 2012. Hyaluronic acid: A key molecule in skin aging. *Dermatoendocrinol,* 4**,** 253-8.

PASONEN-SEPPANEN, S. M., MAYTIN, E. V., TORRONEN, K. J., HYTTINEN, J. M., HASCALL, V. C., MACCALLUM, D. K., KULTTI, A. H., JOKELA, T. A., TAMMI, M. I. & TAMMI, R. H. 2008. All-trans retinoic acid-induced hyaluronan production and hyperplasia are partly mediated by EGFR signaling in epidermal keratinocytes. *J Invest Dermatol,* 128**,** 797-807.

PASSI, A., VIGETTI, D., BURASCHI, S. & IOZZO, R. V. 2019. Dissecting the role of hyaluronan synthases in the tumor microenvironment. *FEBS J,* 286**,** 2937-2949.

PHILIPSON, L. H. & SCHWARTZ, N. B. 1984. Subcellular localization of hyaluronate synthetase in oligodendroglioma cells. *J Biol Chem,* 259**,** 5017-23.

PHILIPSON, L. H., WESTLEY, J. & SCHWARTZ, N. B. 1985. Effect of hyaluronidase treatment of intact cells on hyaluronate synthetase activity. *Biochemistry,* 24**,** 7899-906.

PREHM, P. 1984. Hyaluronate is synthesized at plasma membranes. *Biochem J,* 220**,** 597-600.

PROSDOCIMI, M. & BEVILACQUA, C. 2012. Exogenous hyaluronic acid and wound healing: an updated vision. *Panminerva Med,* 54**,** 129-35.

QUAN, T., WANG, F., SHAO, Y., RITTIE, L., XIA, W., ORRINGER, J. S., VOORHEES, J. J. & FISHER, G. J. 2013. Enhancing structural support of the dermal microenvironment activates fibroblasts, endothelial cells, and keratinocytes in aged human skin in vivo. *J Invest Dermatol,* 133**,** 658-667.

REED, M. J., DAMODARASAMY, M., CHAN, C. K., JOHNSON, M. N., WIGHT, T. N. & VERNON, R. B. 2013. Cleavage of hyaluronan is impaired in aged dermal wounds. *Matrix Biol,* 32**,** 45-51.

RENNEKAMPFF, H. O., HANSBROUGH, J. F., KIESSIG, V., DORE, C., STICHERLING, M. & SCHRODER, J. M. 2000. Bioactive interleukin-8 is expressed in wounds and enhances wound healing. *J Surg Res,* 93**,** 41-54.

RIPPA, A. L., KALABUSHEVA, E. P. & VOROTELYAK, E. A. 2019. Regeneration of Dermis: Scarring and Cells Involved. *Cells,* 8.

ROCK, K., GRANDOCH, M., MAJORA, M., KRUTMANN, J. & FISCHER, J. W. 2011. Collagen fragments inhibit hyaluronan synthesis in skin fibroblasts in response to

ultraviolet B (UVB): new insights into mechanisms of matrix remodeling. *J Biol Chem,* 286**,** 18268-76.

ROCK, K., MEUSCH, M., FUCHS, N., TIGGES, J., ZIPPER, P., FRITSCHE, E., KRUTMANN, J., HOMEY, B., REIFENBERGER, J. & FISCHER, J. W. 2012. Estradiol protects dermal hyaluronan/versican matrix during photoaging by release of epidermal growth factor from keratinocytes. *J Biol Chem,* 287**,** 20056-69.

ROY, B., YUAN, L., LEE, Y., BHARTI, A., MITRA, A. & SHIVASHANKAR, G. V. 2020. Fibroblast rejuvenation by mechanical reprogramming and redifferentiation. *Proc Natl Acad Sci U S A,* 117**,** 10131-10141.

SAAVALAINEN, K., PASONEN-SEPPANEN, S., DUNLOP, T. W., TAMMI, R., TAMMI, M. I. & CARLBERG, C. 2005. The human hyaluronan synthase 2 gene is a primary retinoic acid and epidermal growth factor responding gene. *J Biol Chem,* 280**,** 14636-44.

SAPUDOM, J., MULLER, C. D., NGUYEN, K. T., MARTIN, S., ANDEREGG, U. & POMPE, T. 2020. Matrix Remodeling and Hyaluronan Production by Myofibroblasts and Cancer-Associated Fibroblasts in 3D Collagen Matrices. *Gels,* 6.

SAYO, T., SUGIYAMA, Y., TAKAHASHI, Y., OZAWA, N., SAKAI, S., ISHIKAWA, O., TAMURA, M. & INOUE, S. 2002. Hyaluronan synthase 3 regulates hyaluronan synthesis in cultured human keratinocytes. *J Invest Dermatol,* 118**,** 43-8.

SHIRAKATA, Y., KIMURA, R., NANBA, D., IWAMOTO, R., TOKUMARU, S., MORIMOTO, C., YOKOTA, K., NAKAMURA, M., SAYAMA, K., MEKADA, E., HIGASHIYAMA, S. & HASHIMOTO, K. 2005. Heparin-binding EGF-like growth factor accelerates keratinocyte migration and skin wound healing. *J Cell Sci,* 118**,** 2363-70.

SIMPSON, C. L., PATEL, D. M. & GREEN, K. J. 2011. Deconstructing the skin: cytoarchitectural determinants of epidermal morphogenesis. *Nat Rev Mol Cell Biol,* 12**,** 565-80.

SINGER, A. J. & CLARK, R. A. 1999. Cutaneous wound healing. *N Engl J Med,* 341**,** 738-46.

SMITH, M. M. & MELROSE, J. 2015. Proteoglycans in Normal and Healing Skin. *Adv Wound Care (New Rochelle),* 4**,** 152-173.

SNELL, R. S. 1965. The Fate of Epidermal Desmosomes in Mammalian Skin. *Z Zellforsch Mikrosk Anat,* 66**,** 471-7.

SNETKOV, P., ZAKHAROVA, K., MOROZKINA, S., OLEKHNOVICH, R. & USPENSKAYA, M. 2020. Hyaluronic Acid: The Influence of Molecular Weight on Structural, Physical, Physico-Chemical, and Degradable Properties of Biopolymer. *Polymers (Basel),* 12.

SOLTES, L., MENDICHI, R., KOGAN, G., SCHILLER, J., STANKOVSKA, M. & ARNHOLD, J. 2006. Degradative action of reactive oxygen species on hyaluronan. *Biomacromolecules,* 7**,** 659-68.

SPICER, A. P., SELDIN, M. F., OLSEN, A. S., BROWN, N., WELLS, D. E., DOGGETT, N. A., ITANO, N., KIMATA, K., INAZAWA, J. & MCDONALD, J. A. 1997. Chromosomal localization of the human and mouse hyaluronan synthase genes. *Genomics,* 41**,** 493-7.

STERN, R. 2003. Devising a pathway for hyaluronan catabolism: are we there yet? *Glycobiology,* 13**,** 105R-115R.

STERN, R. 2004. Hyaluronan catabolism: a new metabolic pathway. *Eur J Cell Biol,* 83**,** 317-25.

STERN, R. 2010. *Hyaluronan and the Process of Aging in Skin. In: Farage M.A., Miller K.W., Maibach H.I. (eds) Textbook of Aging Skin,* Berlin, Heidelberg, Springer.

STERN, R., ASARI, A. A. & SUGAHARA, K. N. 2006. Hyaluronan fragments: an information-rich system. *Eur J Cell Biol,* 85**,** 699-715.

STERN, R. & JEDRZEJAS, M. J. 2006. Hyaluronidases: their genomics, structures, and mechanisms of action. *Chem Rev,* 106**,** 818-39.

STERN, R. & MAIBACH, H. I. 2008. Hyaluronan in skin: aspects of aging and its pharmacologic modulation. *Clin Dermatol,* 26**,** 106-22.

STERN, R., SHUSTER, S., WILEY, T. S. & FORMBY, B. 2001. Hyaluronidase can modulate expression of CD44. *Exp Cell Res,* 266**,** 167-76.

STOLL, S. W., RITTIE, L., JOHNSON, J. L. & ELDER, J. T. 2012. Heparin-binding EGF-like growth factor promotes epithelial-mesenchymal transition in human keratinocytes. *J Invest Dermatol,* 132**,** 2148-57.

STRIETER, R. M., PHAN, S. H., SHOWELL, H. J., REMICK, D. G., LYNCH, J. P., GENORD, M., RAIFORD, C., ESKANDARI, M., MARKS, R. M. & KUNKEL, S. L. 1989. Monokine-induced neutrophil chemotactic factor gene expression in human fibroblasts. *J Biol Chem,* 264**,** 10621-6.

SUGIYAMA, Y., SHIMADA, A., SAYO, T., SAKAI, S. & INOUE, S. 1998. Putative hyaluronan synthase mRNA are expressed in mouse skin and TGF-beta upregulates their expression in cultured human skin cells. *J Invest Dermatol,* 110**,** 116-21.

SZE, J. H., BROWNLIE, J. C. & LOVE, C. A. 2016. Biotechnological production of hyaluronic acid: a mini review. *3 Biotech,* 6**,** 67.

TAMMI, M. I., DAY, A. J. & TURLEY, E. A. 2002. Hyaluronan and homeostasis: a balancing act. *J Biol Chem,* 277**,** 4581-4.

TAMMI, R., PAUKKONEN, K., WANG, C., HORSMANHEIMO, M. & TAMMI, M. 1994. Hyaluronan and CD44 in psoriatic skin. Intense staining for hyaluronan on dermal capillary loops and reduced expression of CD44 and hyaluronan in keratinocyte-leukocyte interfaces. *Arch Dermatol Res,* 286**,** 21-9.

TANABE, K. K., NISHI, T. & SAYA, H. 1993. Novel variants of CD44 arising from alternative splicing: changes in the CD44 alternative splicing pattern of MCF-7 breast carcinoma cells treated with hyaluronidase. *Mol Carcinog,* 7**,** 212-20.

TAUB, D. D., ANVER, M., OPPENHEIM, J. J., LONGO, D. L. & MURPHY, W. J. 1996. T lymphocyte recruitment by interleukin-8 (IL-8). IL-8-induced degranulation of neutrophils releases potent chemoattractants for human T lymphocytes both in vitro and in vivo. *J Clin Invest,* 97**,** 1931-41.

TAVIANATOU, A. G., CAON, I., FRANCHI, M., PIPERIGKOU, Z., GALESSO, D. & KARAMANOS, N. K. 2019. Hyaluronan: molecular size-dependent signaling and biological functions in inflammation and cancer. *FEBS J,* 286**,** 2883-2908.

TEZEL, A. & FREDRICKSON, G. H. 2008. The science of hyaluronic acid dermal fillers. *J Cosmet Laser Ther,* 10**,** 35-42.

THULABANDU, V., CHEN, D. & ATIT, R. P. 2018. Dermal fibroblast in cutaneous development and healing. *Wiley Interdiscip Rev Dev Biol,* 7.

TOOLE, B. P. 2004. Hyaluronan: from extracellular glue to pericellular cue. *Nat Rev Cancer,* 4**,** 528-39.

TRACY, L. E., MINASIAN, R. A. & CATERSON, E. J. 2016. Extracellular Matrix and Dermal Fibroblast Function in the Healing Wound. *Adv Wound Care (New Rochelle),* 5**,** 119-136.

TURLEY, E. A., NOBLE, P. W. & BOURGUIGNON, L. Y. 2002. Signaling properties of hyaluronan receptors. *J Biol Chem,* 277**,** 4589-92.

USUI, M. L., MANSBRIDGE, J. N., CARTER, W. G., FUJITA, M. & OLERUD, J. E. 2008. Keratinocyte migration, proliferation, and differentiation in chronic ulcers from patients with diabetes and normal wounds. *J Histochem Cytochem,* 56**,** 687-96.

VAALAMO, M., WECKROTH, M., PUOLAKKAINEN, P., KERE, J., SAARINEN, P., LAUHARANTA, J. & SAARIALHO-KERE, U. K. 1996. Patterns of matrix metalloproteinase and TIMP-1 expression in chronic and normally healing human cutaneous wounds. *Br J Dermatol,* 135**,** 52-9.

VELNAR, T., BAILEY, T. & SMRKOLJ, V. 2009. The wound healing process: an overview of the cellular and molecular mechanisms. *J Int Med Res,* 37**,** 1528-42.

VIGETTI, D., KAROUSOU, E., VIOLA, M., DELEONIBUS, S., DE LUCA, G. & PASSI, A. 2014. Hyaluronan: biosynthesis and signaling. *Biochim Biophys Acta,* 1840**,** 2452-9.

VOLPI, N., SCHILLER, J., STERN, R. & SOLTES, L. 2009. Role, metabolism, chemical modifications and applications of hyaluronan. *Curr Med Chem,* 16**,** 1718-45.

WANG, F., GARZA, L. A., KANG, S., VARANI, J., ORRINGER, J. S., FISHER, G. J. & VOORHEES, J. J. 2007. In vivo stimulation of de novo collagen production caused by cross-linked hyaluronic acid dermal filler injections in photodamaged human skin. *Arch Dermatol,* 143**,** 155-63.

WEBER, G. C., BUHREN, B. A., SCHRUMPF, H., WOHLRAB, J. & GERBER, P. A. 2019. Clinical Applications of Hyaluronidase. *Adv Exp Med Biol,* 1148**,** 255-277.

WEIGEL, P. H. & BAGGENSTOSS, B. A. 2017. What is special about 200 kDa hyaluronan that activates hyaluronan receptor signaling? *Glycobiology,* 27**,** 868-877.

WEIGEL, P. H. & DEANGELIS, P. L. 2007. Hyaluronan synthases: a decade-plus of novel glycosyltransferases. *J Biol Chem,* 282**,** 36777-81.

WEIGEL, P. H., HASCALL, V. C. & TAMMI, M. 1997. Hyaluronan synthases. *J Biol Chem,* 272**,** 13997-4000.

WEST, D. C., HAMPSON, I. N., ARNOLD, F. & KUMAR, S. 1985. Angiogenesis induced by degradation products of hyaluronic acid. *Science,* 228**,** 1324-6.

WYSOCKI, A. B. 1999. Skin anatomy, physiology, and pathophysiology. *Nurs Clin North Am,* 34**,** 777-97, v.

YAMADA, Y., ITANO, N., HATA, K., UEDA, M. & KIMATA, K. 2004. Differential regulation by IL-1beta and EGF of expression of three different hyaluronan synthases in oral mucosal epithelial cells and fibroblasts and dermal fibroblasts: quantitative analysis using real-time RT-PCR. *J Invest Dermatol,* 122**,** 631-9.

YANG, C., CAO, M., LIU, H., HE, Y., XU, J., DU, Y., LIU, Y., WANG, W., CUI, L., HU, J. & GAO, F. 2012. The high and low molecular weight forms of hyaluronan have distinct effects on CD44 clustering. *J Biol Chem,* 287**,** 43094-107.

Acknowledgments

I would like to express my sincere gratitude and thanks to my supervisor Prof. Dr. med. Peter Arne Gerber for guiding me through all steps of this project with patience. He provided me with advice, valuable suggestions, and continuous encouragement.

I am also very grateful to Prof. Dr. med. Bernhard Homey for giving me the opportunity to carry out this fascinating research. I appreciate the interesting discussions and expert scientific guidance.

My special thanks go to Prof. Dr. med. Edwin Bölke for co-advising this work and Prof. Dr. med. Timm Filler for serving as an additional reviewer.

Many thanks are due to Dr. rer. nat. Holger Schrumpf for his help with graphical illustration and comments on the manuscript.

I would like to dedicate my very special appreciation to my family for their constant support and for providing me with endless love, belief, and encouragement.